OPTICAL FIBER SENSOR TO MONITOR PHYSICAL MEASURANDS FOR CIVIL APPLICATIONS

A Thesis Submitted in Fulfilment of the Requirement for the Award of the Degree of

MASTER OF ENGINEERING

in

Electronics and Communication

Submitted by

ISHANT DHINGRA

(801661010)

Under Supervision of

Dr. R. S. Kaler

(Senior Professor)

ELECTRONICS AND COMMUNICATION ENGINEERING DEPARTMENT
THAPAR INSTITUTE OF ENGINEERNG & TECHNOLOGY
(A DEEMED TO BE UNIVERSITY), PATIALA, PUNJAB
JULY, 2018

DECLARATION

I, Ishant Dhingra, hereby declare that the work presented in this thesis entitled **"Optical Fiber Sensor to monitor physical measurands for civil applications"** in fulfillment of the requirement for the award of degree of Master of Engineering (ECE) submitted at Electronics and Communication Engineering Department, Thapar Institute of Engineering & Technology (Deemed to be University), Patiala is an authentic record of work carried out under supervision of Dr. R. S. Kaler (Senior Professor, Electronics and Communication, Thapar Institute of Engineering and Technology). The matter presented in this has not been submitted either in part or full to any other university or institute for the award of any other degree.

Ishant Dhingra

Date: 13 August, 2018

Ishant Dhingra

801661010

Date: 13 August, 2018

Dr. R. S. Kaler

(Senior Professor)

Electronics and Communication Engineering Department

Thapar Institute of Engineering & Technology

(A Deemed to be University), Patiala, Punjab

ACKNOWLEDGEMENT

First and foremost, I would like to express my gratitude and acknowledgement to my M.E. dissertation thesis supervisor **Dr. R.S. KALER** (Senior Professor); who has an attitude and substance of a genius; who has continually and convincingly conveyed a spirit of adventure in regard to research. I would also like to thank him for his useful comments, remarks, motivation and constant support provided throughout this course work.

I also express my heartiest gratitude to **Prof. Prakash Gopalan**, Director, Thapar Institute of Engineering and Technology, Patiala, for providing the resources for my research work. I express my sincere thanks to **Dr. Alpana Aggarwal (Head of Department)** for allowing me to carry out this thesis project.

I proudly grab this opportunity to express my thanks to **Mrs. Gurpreet Kaur** for guiding and supporting me throughout this research project. Without her guidance and persistent help, this project would not have been possible. I am thankful for her valuable engagement and encouragement. I would like to thank my lab mates who have supported me through thick and thin **Ms. Jiwanpreet Kaur**, **Ms. Mukti Yadav**, **Mrs. Madhvi Verma** and **Ms. Tamanna Jain**, who have willingly shared their precious time during this process.

I am highly grateful to my family for standing by my side as a pillar of strength and always pushing me further ahead. I would love to mention my gratitude to my parents **Mr. Tek Dhingra** and **Mrs. Bimla Dhingra**, my loving sister **Ms. Khahish Dhingra** and my grandparents; without their blessings I wouldn't have completed this project.

This acknowledgment is incomplete without thanking the people, I was around during this particular period of time, for hearing me out and keeping me harmonious.

And above all I express my indebtness to the almighty for all his blessings.

ABSTRACT

In the past few years, the fiber bragg grating sensors have offered a great potential for a wide range of applications in many fields. Many bragg grating sensors such as fiber bragg grating sensors, long-period fiber gratings sensors, tilted fiber bragg gratings sensors, chirped fiber bragg gratings sensors have shown high sensitivity, stability, immunity to electromagnetic interference and environmental ruggedness. There has been a noticeable contribution of these bragg gratings-based components in different fields such as biomedical applications for brain pressure monitoring, military applications for guided missiles temperature measurement and civil applications for structural health monitoring. The bragg grating sensors consist of periodic gratings having different grating refractive index. The objective of this dissertation is to design and analyse various optical fiber sensors based on bragg gratings. The transmission characteristics and propagation of waves have been studied with the help of electromagnetic frequency domain to find the wavelength shifts. The study to design fiber bragg grating sensor was carried out with the help of software. The effect of strain on various infrastructure is also analyzed.

Firstly, an optical fiber bragg grating sensor is designed in Comsol software. The performance of fiber bragg grating sensor is enhanced by selecting appropriate material for its fabrication. By introducing desirable refractive index, writing large number of gratings selecting, appropriate dimensions result in wavelength variation at desired value. These modifications are done to achieve enhanced sensitivity and better sensing operations.

Further, we investigated that the proposed fiber bragg grating sensor can also be used to analyze the effect of strain on metal rods (corroded or non-corroded) at different temperature values. The wavelength shift is analyzed to monitor the strength of metal rods. The graphs for different transmission wavelengths revealed that this sensor would be applicable for monitoring the strength of metal pipes used in massive structure and the parameters that effect its strength.

TABLE OF CONTENTS

LIST OF TABLES

LIST OF FIGURES

CHAPTER-1

INTRODUCTION

1.1 OPTICAL FIBER SENSOR

As far back as old circumstances, a standout amongst the most vital needs of individuals has been to impart, which made interest for designing and creating communication system for sending messages starting with one far off place then onto the next. In 1966, Dr. K. C. Kao and his associates in Standard Telecommunication Laboratories Ltd. to begin with presented the idea of directing light with optical fibers [1].

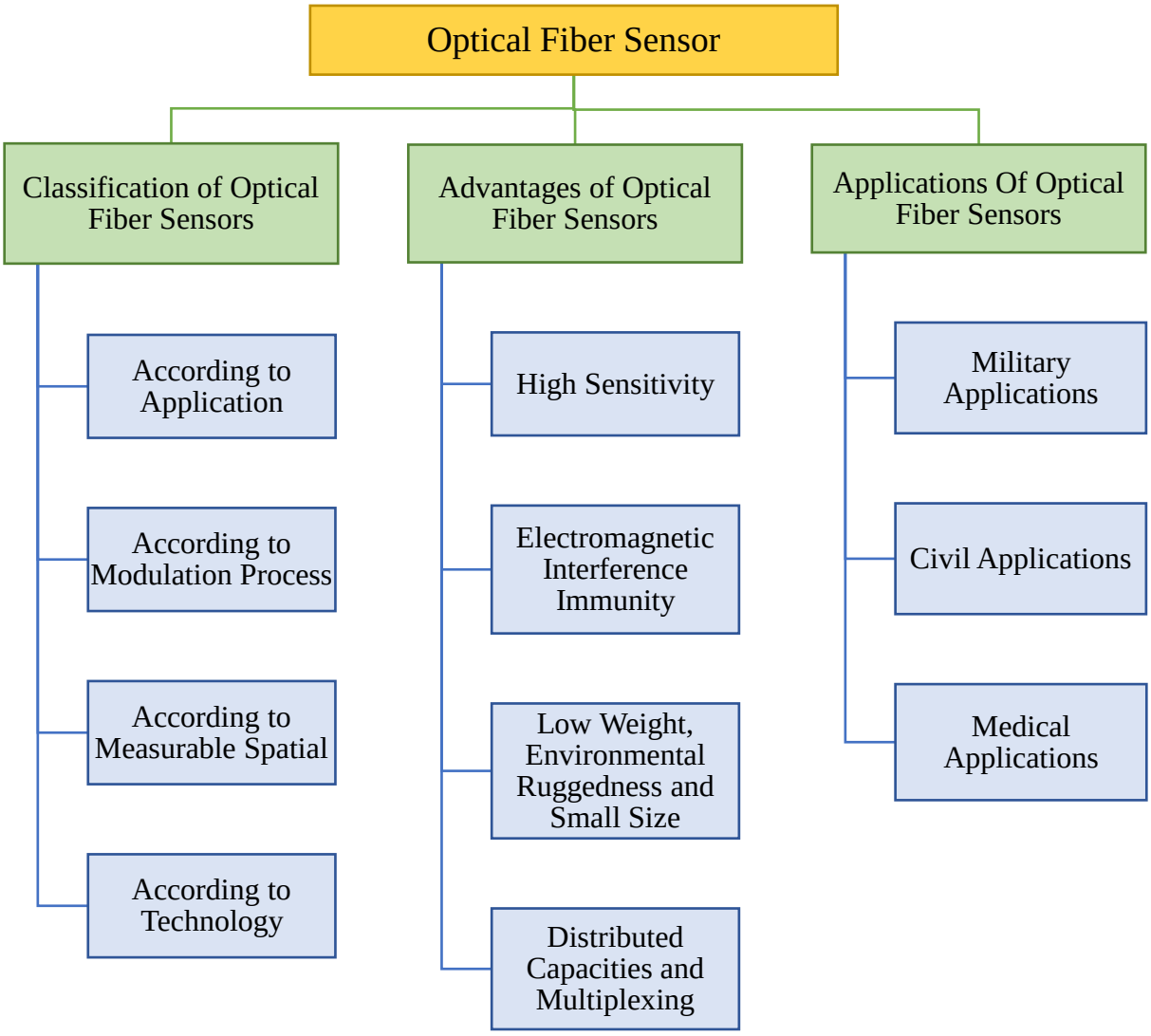

Figure 1.1 Flow chart detailing major features of optical fiber sensor.

Afterward, since the origin of optical fiber communications, optical fibers, which are glass or plastic tube-shaped waveguides that convey light along their length, are key in any communication system everywhere throughout the world. What's more, finished the previous 30 years, another industry, optoelectronics industry has prompted the development of numerous new item regions, including compact laser printers, compact disc player, and personal copiers, and so forth., because of both the quality enhancements and cost decreases in optoelectronic parts [2].

In parallel with these improvements, optical fiber sensors, which have been a main user of the innovation related with the optoelectronics and fiber optic communications ventures, have intrigued the scientists and enticed the application engineers for more than forty years. There is most likely that this innovation can bring an abundance of applications, running from sensors in the medical industry for observing vital biological functions, the aviation and wind-vitality ventures for checking the soundness of the huge structures, through to immense distributed sensors in oil industry. Numerous segments related with optical fiber communications and optoelectronics businesses are created for optical fiber sensor applications these days. The capacity of optical fiber sensors to dislodge customary sensors for detecting applications has been upgraded, since segment costs have fallen and the segment quality has been enhanced greatly.

1.2 APPLICATIONS OF OPTICAL FIBER SENSORS

The recent advancements in the fiber sensors industry have made it possible for us to estimate and calculate various distinct parameters. To date, in excess of 70 distinct parameters could be estimated or checked by optical fiber sensors, for example, temperature, speeding up, stress, electric and attractive fields, rotation, weight, thickness, refractive index, strain, stickiness, vibration, acoustics, and so on. Optical fiber sensors have turned out to be increasingly essential, and in many industries, they step by step wind up imperative, for example, in military, medicinal and civil applications.

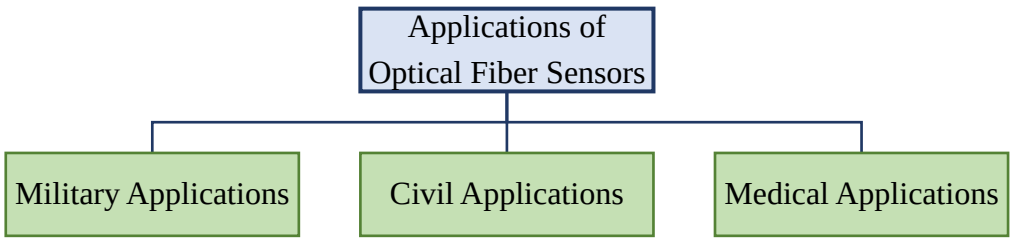

Figure 1.2 Applications of optical fiber sensors.

1.2.1 Military Applications

The use of optical fiber sensors in military applications have gained a lot of popularity owing to their ability to give details for rotational rate. Fiber optic gyroscope (FOG) is name given to the sensors which details rate for rotational data [3]. The operating and functioning of FOGs is based on of the principle of Sagnac effect, which deals with rotationally elicited evoked interferences [4]. The

application of FOGs as a heading sensor in navigation systems has been feasible since 1995 in luxury sedans of Nissan motor company [5]. These days, FOGs give the prevailing arrangement in many practices, for example, control, and stabilization of missiles, automobiles, navigation, attitude heading and reference system, satellites, guidance, robotics, and so forth [6,7].

The use of acoustic sensors in the military applications for detection has been in scene from past decades. Optical fiber hydrophone had been created for military usage long ago. In this sensor, the optical fiber functions as a detecting component, making it function as an acoustic sensor. The advancement of optical fiber hydrophone began in the late 1970s [8,9]. The United States built up their fiber optic hydrophones utilized as a part of the Navy ships for submerged investigation since 1990. Other than the military applications, optical fiber hydrophones could likewise be utilized for geophysical applications, for example, seismic investigation for oil reservoirs.

1.2.2 Civil Applications

As a matter of first importance, optical fiber sensors have turned out to be important tool in the oil and gas industry, helping engineers to find and screen the wells, as well as concentrate the biggest conceivable level of oil and gas out of them. The environmental conditions inside the gas or oil wells are challenging with temperature more than 100 ^{o}C or even when inflated to 200 ^{o}C [10]. Under such severe environment, consistency of these conventional electrical sensors has been found to be reduced to a certain level. This limitation has been overcome by optical fiber sensors, owing to their passive nature. The inborn nature of optical fiber sensors has made it possible to use them in gas and oil industry as well. These sensors have simple fiber as their detecting component so the light need not to make re-entries into the fiber core. These particular sensors have made potential applications in exploring the geophysical properties of formation of rocks. Nowadays, it has been made possible to track the separation process of gas, oil and water.

Besides, optical fiber sensors could likewise discover applications in checking integrity and buckling of pipeline [11], pointing defects in wall-thinning [12,13,14], or to aim at leakage in pipelines [15]. The national and international transportation of gases and fluids is done through the pipelines; so, any let-down in pipeline networks could cost a nation heavy financial and economic losses in addition to fierce environmental effects. Therefore, it is essential to keep an eye on pipeline integrity and strength throughout the network. To cite an illustration, Italy scientists have exhibited the use of optical fiber sensors in screening any deformation of soil or rock nearby the pipeline and checking pipeline's structural integrity [16]. An exploration bunch from Canada utilized the conveyed fiber sensor in identifying restricted divider locking in an energy pipe by estimating the longitudinal and the loop strain circulations through the external pipe surface [11]. They also exhibited utilization of the comparable procedure in distinction of few cutouts in inner wall by estimating hoop and pivotal strain distributions along the external surface using an end-capped steel pipe. These innovations have just infiltrated into

the practical market and trading, since they have accomplished spatial determination in centimeter range across several kilometers estimation extend [17,18,19,20]. This marketing of optical sensors has made them quite popular. They are relied upon to assume an essential part in the pipeline enterprises to spare cash for examination and upkeep.

Figure 1.3 Applications of optical fiber sensors: turbine blades.

The health of wind-turbine edges, aircrafts, dams and spans i.e. of enormous structures is to be checked constantly, so that a strategic distance from some catastrophe mischances can be maintained. For instance, scientists in Germany have tried Bragg grating based optical fiber sensors by planting them in the tail of the new Airbus A340/600. The potential of these sensors is currently examined on the A380 [21]. The opportunity to draft investigation, health and then retirement of aircraft to eliminate any mis happenings is provided by these sensors; as when engraved into an aircraft structure they readily measure strain in the view of real loads experienced. Moreover, these optical sensors have been used extensively, to monitor wind-turbine blades health. Since, the wind turbines are growing in size resulting in new designing complications, optical fiber sensors could give an idea of loads in real-time and history of blade history, which is helpful for both the makers and wind-farm proprietors.

In addition, optical fiber sensors have gained up surging interest in numerous civil applications, for example, analysing movement effect on concrete pieces [22], recognizing hydrogen leaks [23], intrusion [24,25], vibration [26,27,28], and so forth.

1.2.3 Medical Applications

As the optical fiber sensors could be manufactured in a concise and compact size, they have gained much interest from the bio-medical field, particularly in the development of insignificantly intrusive surgical tools. One of the sensors extensively used in medical field is miniature pressure sensor, used for intracranial pressure observing in neurology [29]. Likewise, the sensors could be placed on

instrumented catheters' tip so that simultaneous measurement of strain and temperature could take place; helping in planning if surgical strategies.

The medical applications where optical fiber sensors have proved to be of excellent use include estimating various parameters, for example, chemical detecting is emerging as developing business sector. For instance, optical fiber sensors that could sense dissolve oxygen and carbon dioxide or pH are currently commercially accessible. Besides, since optical fiber sensors are resistant to electromagnetic obstruction, they are splendidly appropriate for applications including high electromagnetic field, for example, in magnetic resonance-imaging systems.

By contrast, optical fiber biosensors have gained much popularity in medicinal applications, by estimating reflectance, absorbance, fluorescence, etc. for detecting a specific biological species [30]. For instance, the least complex optical biosensors utilize absorbance estimations to decide any adjustments in the grouping of analytes that ingest a given wavelength of light. A fiber optic pH sensor [31] and a fiber optic oxygen sensor [32] have been created for use in medical applications. Likewise, Piunno et al. [33,34] revealed one of the principal biosensors for coordinate investigation of DNA hybridization by utilization of an optical fiber, and specialists in Virginia Institute and State University built up a micro gap fiber multicavity Fabry-P'erot sensor for biosensing [35].

1.3 ADVANTAGES OF OPTICAL FIBER SENSORS

Optical fibers have proved to be beneficial in each and every aspect our lives and have become a hot topic of research both in academic and research fields. The customary electro-mechanical sensor systems have already been popular for quite a period of time, and they have been demonstrated moderately accurate records and sensible assembling costs; in this manner, the fiber-based sensor systems need to show better preferences all together than infiltrate into the market to supplant the current traditional sensors. The points of interest which keep optical fiber sensors survival incorporate high sensitivity, electromagnetic interference immunity, low weight, environmental ruggedness, small size, multiplexing and distributed capacities.

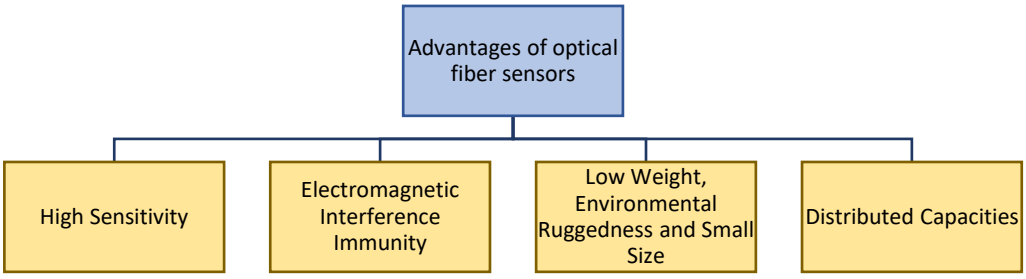

Figure 1.4 Advantages of optical fiber sensors.

1.3.1 High Sensitivity

High sensitivity is the main feature of optical fiber sensors. Since by estimating the difference in the light signal, for example, the wavelength, intensity, phase, and so on., with optical fiber sensors it is easy to attain high sensitivity. Usually, any little disturbance occurring in the surrounding environment has ability to influence the properties of the optical fiber, for example, length, refractive index and design at that point, any such adjustments influence the circumstances under which the light spreads inside the fibers. Even a tiny alteration in surrounding environment would bring about an extensive difference in the light signal by appropriately outlining the sensing head of system.

1.3.2 Electromagnetic Interference Immunity

Glass or other plastic material are generally used in manufacturing of optical fiber. As a large portion of fiber sensing heads are the unadulterated fiber having zero electrical circuits, the outer electromagnetic disturbance influence does not impact the manner by which light is spreading inside the fibers. Optical fiber sensors are found to be fundamentally independent towards the electromagnetic interferences, attributing to the fact that photons act as carriers of sensing data instead of electrons. These photon carriers provide the biggest benefit to the optical fiber sensors in contrast with their electronic counterparts. For instance, radiofrequency, electrical or microwave instruments can make electromagnetic interference in the medicinal working condition. Optical fiber sensors working in this condition could be made significantly littler than the electrical sensors, since they don't should be protected. The smaller than usual size is likely a standout amongst the most critical worries in the space-compelled and instrument-swarmed medical environment

1.3.3 Low weight, Environmental Ruggedness and Small Size

The diameters of optical fibers are in the order of few millimeters and are extremely light in weight. These advantages made it possible to effectively install optical fiber sensors into the structures under observation. The optical fiber sensors are capable of working well under tough conditions, owing to glass materials used in their manufacturing, as glass accounts for extremely stable compound. As an instance, in oil wells, the high temperature conditions and the humidity does not permit tasking of the electrical devices in long run. Moreover, the passive nature of optical fiber sensor makes them significantly more secure when observing is required in the oil well over a long period of time. in such cases the use of conventional electrical devices may give catastrophic results. Optical fiber sensors seems to be the best decision for submerged applications in light of their stability, and zero requirement of other refined water-proof systems to screen the detecting head.

1.3.4 Distributed Capacities and Multiplexing

The optical fiber sensors have just seemed to have a major take over in the race with traditional sensors, which assigns to their distributed capacities and multiplexing. For structural health monitoring applications for wind turbines, dams, pipelines and bridges; sensing devices are required, which could

be able to continuously observe and record the massive structures over long distance. Furthermore, the sensors must be able to locate the specific area where a strain has been amassed or the position that has got disfigured. For such applications optical fiber sensors are good contenders.

To form mesh one arrangement is to cascade point sensors, and after that implant this point sensor web to the massive structures to accomplish the quasi-distributed sensing. An elective arrangement is to utilize light in an optical fiber to acknowledge such fascinating implementations. The principle preferred standpoint of such distributed sensors is their basic sensing head and each could accomplish completely distributed sensing for the case that the positions which should be observed are not known. Till now, the determination of such sensors spatially has been accomplished to centimeter range, and the estimation range could be accomplished up to tens of kilometers, found adequate for the vast majority of the applications.

1.4 CLASSIFICATIONS OF OPTICAL FIBER SENSORS

To date, a gigantic measure of optical fiber sensors have been effectively created and discover their way toward the "real-world" applications. Essentially, optical fiber sensors comprise of four noteworthy segments: optical source, detecting head, signal waveguide (e.g., optical fiber) and detector (see Fig. 1.5).

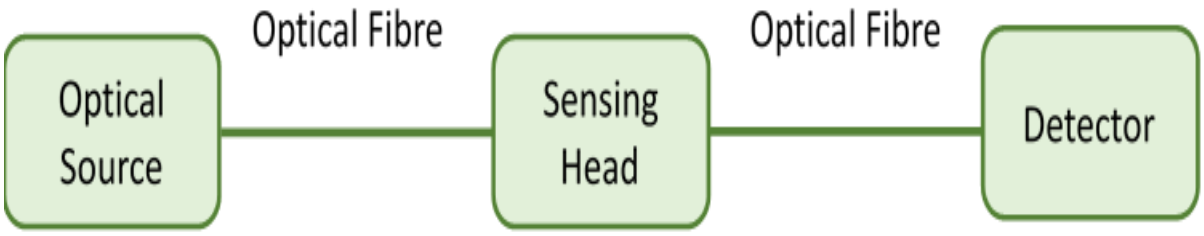

Figure 1.5 Configuration of basic optical fiber sensor consisting of optical source, optical fiber, sensing head and detector.

Light transmits along an optical fiber going through the detecting head, where certain properties of the light wave would be tweaked when the detecting head is impacted by the outer parameters which should be checked. The detector is used to receive the modulated light wave (containing the information) and after the demodulation, the outside shifting parameters which should be estimated could be acquired.

Various types of optical fiber sensors are available in the market and are categorized on the basis of their use in a particular field. The optical fiber sensors are classified as according to the application, type to modulation process, according to measurable spatial scope and on the basis of technology in the respective field. The classification of optical fiber sensor is shown in figure 1.6.

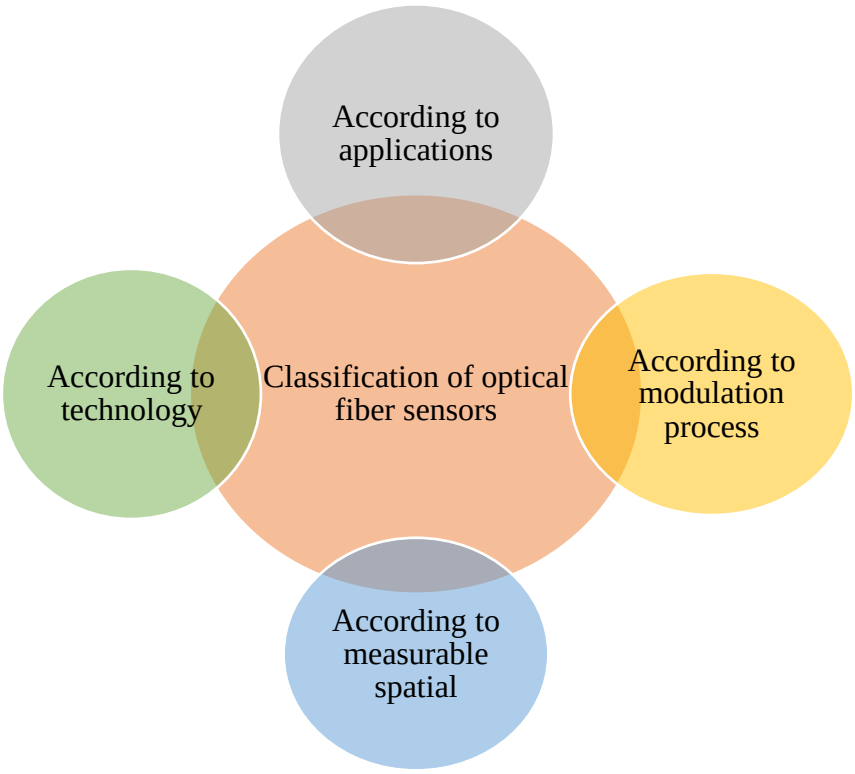

Figure 1.6 Classification of optical fiber sensors.

1.4.1 According to Application

As indicated by various parameters the sensor could measure, or as per diverse applications, optical fiber sensors could be classified as strain sensors, temperature sensors, current sensors, vibration sensors, pressure sensors, chemical sensors, and so on. To categorize the fiber sensors this is a straightforward method. The clients could classify the optical fiber sensors effectively to meet their necessities. For the majority of the optical fiber sensor fabrication, they publicize their sensor products in order to become "user-friendly" in accordance with applications.

1.4.2 According to Modulation Process

Propagating of light wave along optical fiber could be considered in terms of four factors, which are wavelength (frequency), phase, intensity and state of polarization. At the point when the surrounding environment has certain disturbance on the sensing head, no less than one of the four factors change as indicated by the impact. By estimating variation in light signal, one could acquire the helpful data of the surrounding environment change. In this manner, optical fiber sensors could be categorized according to the modulation process as phase modulation sensors, intensity modulation sensors, wavelength modulation sensors, as well as polarization modulation sensors.

1.4.3 According to Measurable Spatial Scope

Optical fiber sensors could also be divided as quasi-distributed sensors, point sensors, and fully distributed sensors. The benefit of optical fiber sensors is that they could be created with a small size,

and these point sensors could be utilized to sense the constraints of numerous points in the space. For instance, in medical application, the information of temperature and pressure inside certain tissues are vital which should be observed amid the surgery. Because of the smaller size of optical fiber sensors, they turn out to be increasingly essential in such applications. Numerous optical fiber components could fill in as point detecting head, for example fiber Bragg gratings (FBGs) [36], optical fiber Fabry- Pérot interferometers [37], multimode fiber interferometers [38], etc.

Quasi-distributed sensors have the ability to detect the parameters of various separate points in the space at the same time, by multiplexing the direct sensors toward shape a detecting network. For example, if people are attentive in specific points on various huge structures, or only some locations should be observed, by space division multiplexing FBGs, and putting the FBGs on these locations, all the variations one these points could be observed all the while. This could be accomplished because the detecting data is set converted directly into the wavelength, which is an outright parameter. Numerous quasi-distributed sensing functions with FBG arrays have already been described, but with diverse demodulation method, for example using acousto-optic filters [39], Fabry-Pérot filters [40,41], and FBG-based filters [42], etc.

Despite, for observing the health of various enormous structures, the areas which should be observed are normally not known. This needs the sensors to have the capability for fully distributed sensing, by inserting the sensing fiber into the structure. Despite point sensors could understand quasi-distributed sensing, their limited nature just gives deficient data about the structure health. Consequently, there is requirement for a strategy that detects the faults and evaluates the seriousness of harm of the entire structure. Such a sensor must do fully distributed strain and temperature estimations more than a few meters to several kilometers. Fully distributed fiber sensors, which depend on Rayleigh scattering [43], Raman scattering [44] and Brillouin scattering [45], could understand this purpose. For instance, the method in light of Brillouin scattering called Brillouin Optical Time Domain Analysis (BOTDA) demonstrates great element to knowledge health monitoring of the enormous structures and has just been commercialized.

1.4.4 According to Technology

Another simple method to classify optical fiber sensors is as indicated by various technologies, for example, fiber grating sensors, Fabry-Pérot interferometer sensors, high birefringence fiber loop mirror sensors, polarization-optical time domain reflectometry (P-OTDR) sensors, BOTDA sensors etc. Since there are number of technologies these days which could discover perfect applications as optical fiber sensors, it is difficult to list them all. In spite of most of these technologies are outstanding, with the goal that the technologies which are closely associated to this thesis is presented in the succeeding part.

Further, optical fiber sensors can also be approximately assembled into three fundamental classifications referred to as extrinsic, evanescent and intrinsic sensors.

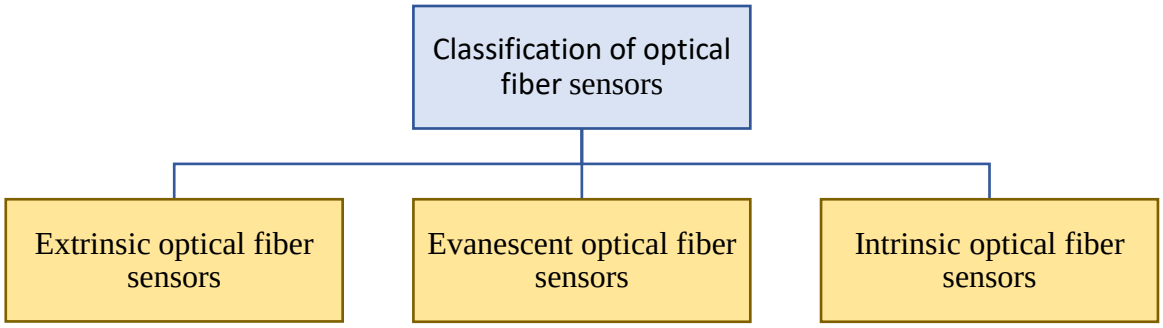

Figure 1.7 Types of optical fiber sensors

For **extrinsic sensors**, the detection of light wave takes place in outside region of fiber. Fig. 1.9 demonstrates the instance of an extrinsic optical fiber sensor. The optical fiber paves the way to a purported "black box" which influences data which should be checked onto the light beam in light of environmental impacts. An optical fiber at that point controls the light with the data impressed by the nearby condition back to detector [2]. Note that the "black box" for the most part contains other electrical or optical gadgets; thus, the extrinsic sensors additionally allude to as hybrid optical fiber sensors.

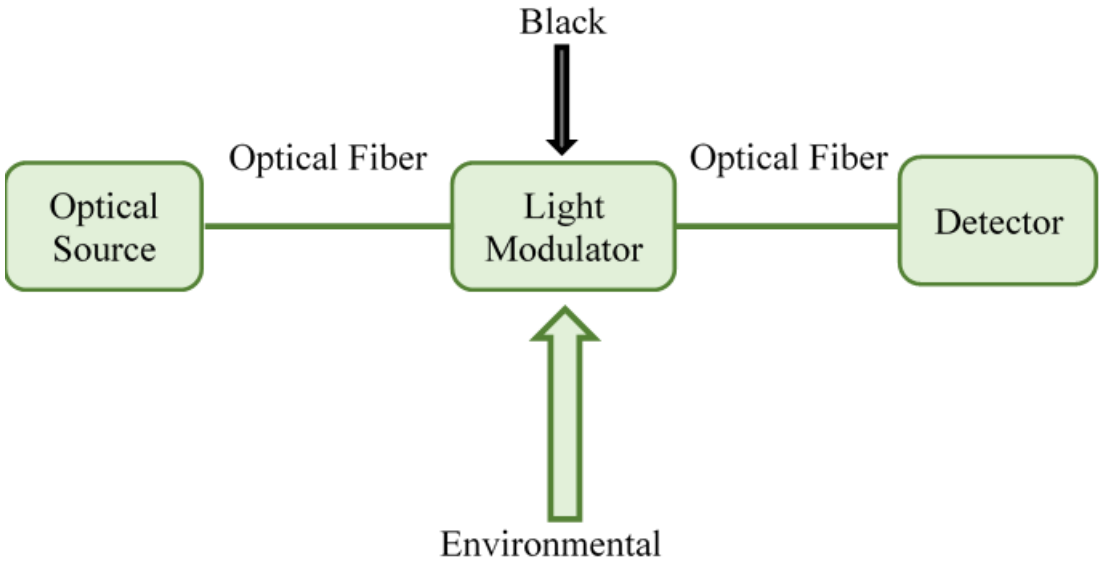

Figure 1.8 Extrinsic type fiber optic sensor.

Evanescent sensor components depend on the quantifiable loss of guidance from an optical wave-guide from a means of sensing outside changes. For example: detection of specific gravity, in recognising chemical spices, in detection of chemical reaction and $P_{H.}$ The effects of micro-bending on optical fiber can also endorse light loss from optical wave-guide and helps in monitoring strain. Here, light is still retained within the overall fiber of structure i.e. light radiation is sustained by cladding layer, that's why it can be classified under the category of intrinsic sensor.

For **Intrinsic sensors**, at least one of the physical properties of the fiber experience a change under environment change. At the end of the day, the intrinsic optical fiber sensor utilizes an optical fiber to convey the light beam, and the environmental impact impresses data onto the light beam while it is in the optical fiber. The outline appeared in Fig. 1.7. The intrinsic optical fiber sensors could likewise allude to as all-fiber sensors.

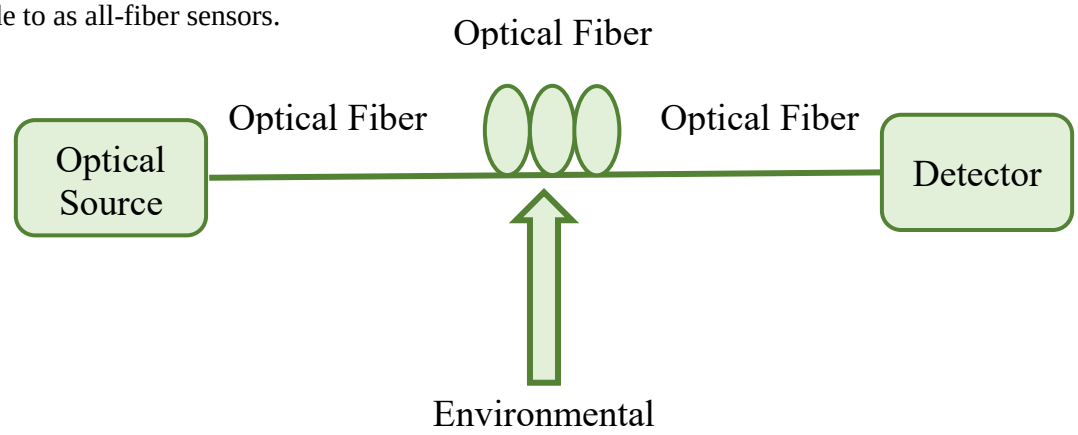

Figure 1.9 Intrinsic type fiber optic sensor.

In any case, there are numerous other characterization strategies for optical fiber sensors so as to be advantageous to clients, researchers, or engineers. Since there is an assortment of types of optical fiber sensors, it is difficult to create a very inclusive illustration. The associated subsections just present some basic categorizations.

1.5 FIBER GRATING SENSORS

The fiber gratings are basic, intrinsic detecting components, which are generally photo-carved into a silica fiber. Generally, they own all the benefits that are ascribed to fiber optical sensors. In further delineation, the core of an optical fiber is built with periodic structure and it will reflect a particular optical wavelength, which is reliant on the periodicity. Shifting in periodicity causes difference in the wavelength. Since this period relies on environmental temperature and remotely connected strains and pressures, we have the reason for a simple sensor (e.g., a fiber grating) which could be effortlessly cross examined. The point by point fabrication of the fiber grinding and intrigued peruses had been discussed in detail in Ref. [46,47,48,49,50,51,52]. The categorisation of the fiber gratings, the detecting principle and additionally the interrogation techniques will be discussed in detail in the following paragraphs.

1.5.1 Classification of Fiber Gratings

Nowadays, a numerous type of fiber gratings are available and as a whole they could be taken as two key types, uniform and nonuniform gratings. The classification of fiber bragg gratings is described in the following flow chart as shown in figure 1.10.

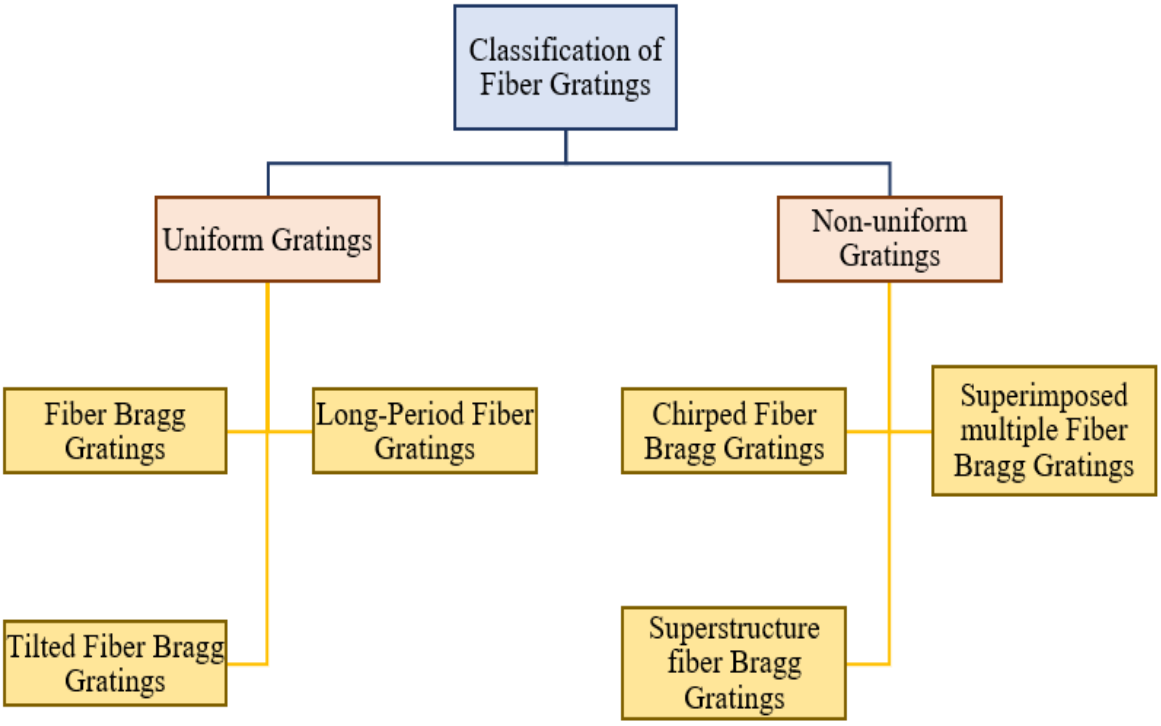

Figure 1.10 Classification of fiber gratings.

1.5.2 Uniform Gratings

In uniform gratings, refractive index possesses a constant modulation depth and gratings are uniform along the axis of fiber core. There are three types of uniform gratings which are categorised on the basis of direction of refractive index variations and the length of the grating pitch. These gratings are named as: fiber Bragg gratings (FBGs), long-period fiber gratings (LPGs), and tilted fiber Bragg gratings (TFBGs).

1.5.2.1 Fiber Bragg Gratings

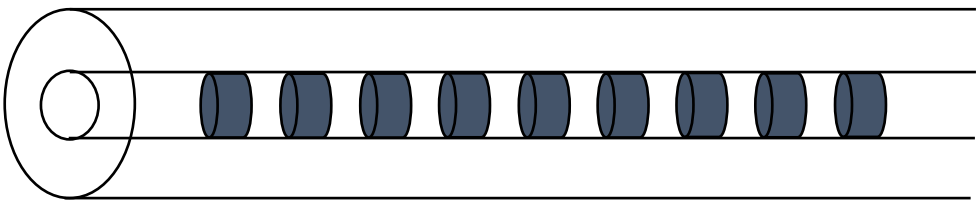

Figure 1.11 Fiber Bragg gratings with uniform variation in refractive index.

The modulation depth of refractive index and periodicity of the FBG are 10^{-5} – 10^{-3} and 100 nm respectively. The changes in refractive index along the direction of optical fiber core axis as shown in figure. For most sensor applications, the wavelength bandwidth relies on particularly grating length

which is around 0.5nm to 0.3nm. In optical communications, FBGs could also find applications such as add-drop multiplexers, wavelength division multiplexing [53], etc. The principles of various FBGs are talked about in the following subsection.

1.5.2.2 Long-Period Fiber Gratings

In 1995, LPGs were generally differentiated in terms of length of the periodicity by Vengsarkar *et al.* [54]. A typical LPG is about 1-3 cm long and possess index modulation depth of 10^{-4} or greater [55]. In contrast to FBGs, the period of LPGs is much larger than the wavelength. It makes LPGs manufacturing simple as compared to FBGs manufacturing. The principle of LPG is that it couples the light out from core into the cladding where it is lost due to scattering and absorption.

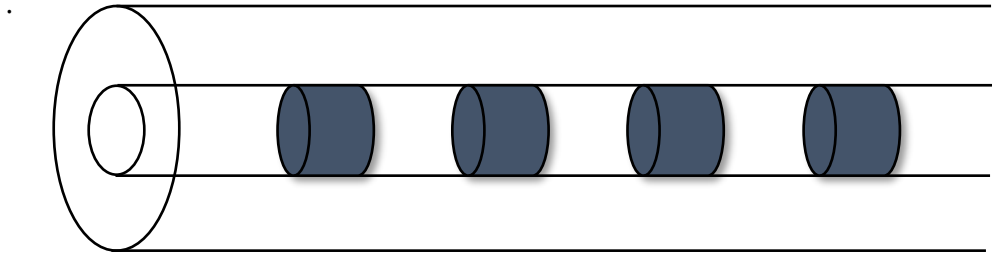

Figure 1.12 Long-period fiber gratings

Initially the LPGs found applications as band-rejection filters [56]. LPGs have also been used as gain-flattening of erbium-doped fiber amplifiers [57]. The resonance wavelength of the LPG is decided by index difference between core and cladding. Hence large wavelength shifts in the resonance can be observed by any changes caused by temperature, strain or even change in external refractive index [58,59,60].

1.5.2.3 Tilted Fiber Bragg Gratings

These are also named as slanted gratings or blazed gratings. Tilted fiber Bragg gratings have periodical index variations in axial direction. The boundary surface of varied index has a certain angle with respect to the fiber axis. Due to certain angle in varied index, it offers some particular characteristics to tilted fiber Bragg gratings. One feature of tilted fiber Bragg gratings is coupling of guided-modes with copropagating modes or counterpropagating modes in specific wavelengths which makes tilted fiber Bragg gratings to be used as gain flattened erbium fiber amplifiers, optical spectrum analyzers, add-drop filters, etc.

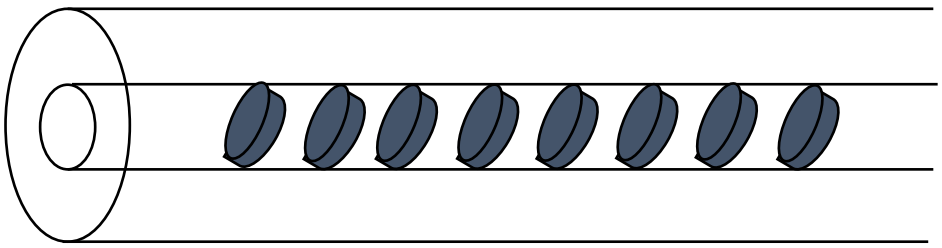

Figure 1.13 Tilted fiber Bragg gratings

The sensitivity of tilted fiber Bragg gratings towards the surrounding refractive index outside the gratings, makes it possible to use them as concentration meters and refractometers. The large tilt angles in tilted fiber Bragg gratings provides good sensitivity to the polarization state of the incident light. Therefore, tilted fiber Bragg gratings can be served as twist sensors, polarimeters, and polarization-dependent loss equalizers. In optical fiber sensors, the applications of TFBGs are to measure strain, temperature, refractive index, bending, vibration etc.

1.5.3 Non-uniform Gratings

Here, the non-uniform periodicity of gratings along the axis of optical fiber core exists. The modulation depth of refractive index need not to be necessarily constant. Several kinds of non-uniform gratings are found in practical world. For instance: chirped fiber Bragg gratings (CFBG), superimposed multiple fiber Bragg gratings (SMFBG), and superstructure fiber Bragg gratings (SFBG).

1.5.3.1 Chirped Fiber Bragg Gratings

To tackle dispersion compensation in high bit-rate telecommunication systems, chirped fiber Bragg gratings were originated. [61]. A single chirp is attained by directly varying the average index, period of grating or both along the length of the grating (see Fig. 2.4).

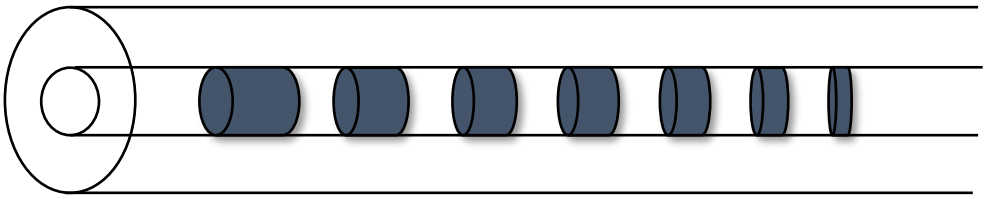

Figure 1.14 Chirped fiber Bragg gratings.

The manufacturing of chirped gratings is done by tapering a fiber into the region of the grating [62]. The effective refractive index along the length of the taper is decreased by reducing core size, bringing about a chirp. In an additional techniques strain gradient is formed across the grating length by bonding an unchirped grating to a substrate with a “soft glue”. The differential shear strength of the glue is held responsible for formation of this strain gradient [63]. Chirped fiber Bragg gratings act uniquely in the existence of strain and temperature fields. In principle, gadgets based on this technique can be wielded to gauge strain and temperature concurrently via deliberately calibrating and monitoring variation in grating spectrum i.e. broadening and shifting at the same time [64].

1.5.3.2 Superimposed Multiple Fiber Bragg Gratings

These multiple gratings allude to a few Bragg gratings engraved in a similar area on an optical fiber [65]. These particular gratings are now vastly used field of in fiber communications, lasers and sensor systems, in light of the fact that multiple Bragg gratings at a similar area fundamentally play out as a comb function and this gadget is in a perfect world appropriate for multiplexing and demultiplexing signals. When a few Bragg gratings are superimposed at a similar area of an optical fiber; then this

arrangement results in reduced individual grating reflectivity, and variation in the Bragg wavelength is observed attributing to the fact that effective refractive index has also shifted. In spite of the fact that 70% reduction is faced by the reflectivity of an individual grating after 7 gratings are superimposed [66], every one of the gratings at a similar area offer new doors into optical integrated technology, as the size of system has to be checked accordingly.

1.5.3.3 Superstructure Fiber Bragg Gratings

A superstructure fiber Bragg grinding alludes to a grinding fiber structure manufactured with an adjusted presentation over the length of the gratings [67]. Along these lines, the Bragg grinding superstructure has an intermittently shifting envelope of the refractive list tweak. The reflection range of such superstructure gratings demonstrates a progression of frequently dispersed peaks, providing additional degrees of opportunity which can be abused in the plan of grinding based gadgets. These superstructure gratings can be utilized as look over channels for flag handling, and for expanding the tunability of the fiber laser-grinding reflector.

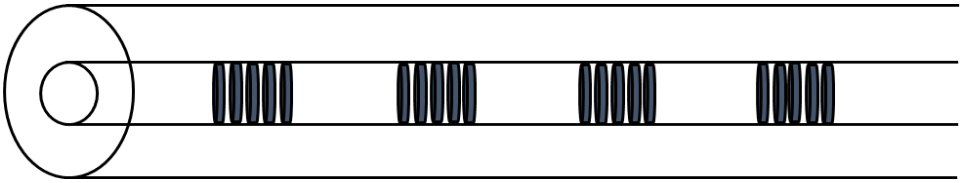

Figure 1.15 Superstructure fiber Bragg gratings.

For various applications, there are numerous different sorts of gratings, for example, composing gratings in multimode fibers, birefringent fibers [68], in the splice point of two unique fibers [69,70]. It is difficult to list all the fiber gratings; in any case, the standards of various types of gratings are comparable. In Section 1.3.4, the basic principle of the FBG is presented, with the goal that the standards of other various types of fiber gratings could be comprehended.

1.5.4 Principle of Fiber Bragg Grating Sensor

The fabrication of Fiber Bragg Gratings is done by exposing the core of single-mode fiber (SMF) to a periodic pattern of intense ultraviolet light.

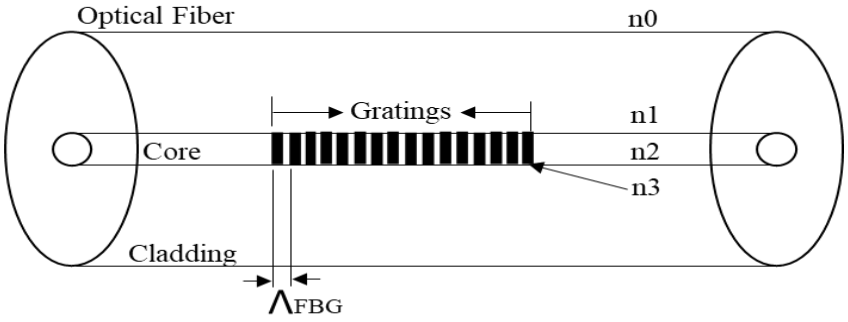

Figure 1.16 Fiber Bragg grating sensor

Fiber Bragg Gratings are made by laterally exposing the core of a single-mode fiber to a periodic pattern of intense ultraviolet light. The exposure produces a permanent increase in the refractive index of the fiber's core, creating a fixed index modulation according to the exposure pattern. This fixed index modulation is called a grating.

At each periodic refraction change a small amount of light is reflected. All the reflected light signals combine coherently to one large reflection at a particular wavelength when the grating period is approximately half the input light's wavelength. This is referred to as the Bragg condition, and the wavelength at which this reflection occurs is called the Bragg wavelength. Light signals at wavelengths other than the Bragg wavelength, which are not phase matched, are essentially transparent.

$$\lambda_B = 2 \times n_{eff} \times \Lambda \tag{1.1}$$

where Λ refers to grating periodicity, λ_B indicates Bragg wavelength and n_{eff} is the effective refractive index.

1.6 THESIS CONTENT SUMMARY

The thesis has been unified into four chapters. The goal of every section is characterized succinctly as follow:

Chapter 1 the basic information of optical fiber sensor have discussed. Classification of fiber sensors, advantages and their applications have included in this chapter. The types of optical fiber sensors based on gratings have also been explained.

Chapter 2 converses the literature survey for understanding the concepts of bragg grating based fiber sensors as well as to describe the main objectives of dissertation.

Chapter 3 focusses on designing of fiber bragg grating sensor with high sensitivity. Further, the designed fiber bragg grating sensor is used to monitor the effect of strain on wavelength at different temperature values.

Chapter 4 of the thesis presents the experimental work of fiber bragg grating sensor to measure strain on different metal rods (corroded and non-corroded).

Chapter 5 presents the future scope in the field of fiber bragg grating sensor to enhance its performance and to use it for monitoring physical measurands for civil applications.

CHAPTER-2

LITERATURE REVIEW

2.1 INTRODUCTION

Fiber Bragg gratings sensor at present is most extensively studied topic in fiber optic technology on account of its intriguing applications in biomedical, military, radar systems, drone missiles and structural health monitoring. The behaviour of FBG sensor makes it unique and appealing product in the market owing to its distinct features like high sensitivity, stability, can withstand harsh conditions and immune to electromagnetic/ radiofrequency interferences. All these properties vary in accordance with surrounding temperature, grating length, core material and its dimensions. The conventional optical fiber sensors were not very stable, accurate and had low sensitivity. So, the researchers are focused on developing a feasible, concise, stable, low cost sensor, high sensitivity which could be able to sense strain and temperature concurrently. The sensors that have been fabricated in the past years have been studied thoroughly and the recent trends have been reviewed below:

2.2 LITERATURE REVIEW OF OPTICAL SENSORS

Asahia et al. in 2009 fabricated an optical fiber sensor consisting type I and pre-strained fiber gratings engraved in a Germania doped silicate fiber. The as- fabricated sensor proved to be concise and compact along the trouble-free execution. It responded linearly on the usage of a simple interrogation system. The strain to temperature response ratio was concluded to be 6%, showed alteration with rise in pre-strain in second type fiber gratings. This fiber Bragg grating (FBG) sensor clearly exhibited distinction in strain and temperature.

Kerrouche *et al*. in 2009 demonstrated a model in which six fiber Bragg grating (FBG) sensors were used consecutively with an array spacing of 60 mm in an optical network for strain measurement. The Bragg grating sensor was embedded inside CFPR (carbon fiber polymer reinforcement) rod. CFPR rods have potential application in concrete structures for reinforcement. A pulling machine was used in order to apply calibrated force and in addition, strain gauge was fixed to get effective results of strain measurements. Calculation from strain to sheer stress revealed uniformity in distribution of throughout the bar. The obtained results proved that these types of systems would be beneficial in structural reinforcement process as they accurately measured *in situ* strains on CFPR rods. The calculation of sheer stress in-between the tendon and wedges has been possible by using the measured strain results obtained from this model.

Hwang *et al.* in 2010 revealed improvised technique to deduce mechanical impacts from the neighbourhood cement of the respective fiber grating in a sensor system. A couple-mode theory ground computation was done to suggest improved bonding in the FBGs in experimental setup, voltages were obtained from filtered spectral power interrogator, instead of optical spectral analyser used in traditional

bonding methods. Reflection peaks were found to be displaced and disturbed in case of glued fiber gratings, glue-free gratings experienced no strain gradient, resulting in a straight-line graph between voltage and average strains. Further calibrations were done in this system using resistance strain gauge.

Comanici *et al*. in 2011 proposed a laser-based fiber Bragg grating (FBG) sensor system to calculate dynamic strain experienced by ceramic piezo-electric transducer (PZT) of cylindrical geometry. An increase in output power and a narrowing bandwidth of reflection signal, were observed as major upgradations in this laser-based sensor. Wavelength-to-power mapping technique was used to demonstrate static and dynamic strain changes. The experimental setup included semiconductor optical amplifier and FBG sensor placed on PZT. DC and sinusoidal voltages were applied to PZT to measure steady-state and dynamic strains, respectively. A linear response recorded between Bragg wavelength and strain proved the system capable for recording dynamic (up to 2 MHz) strain measurements.

Shinoda *et al*. in 2011 presented a model to measure real-time static strain with the help of fiber Bragg grating (FBG) sensor with optical frequency domain reflectometry (OFDR). The reflected wavelengths of multipoint FBGs could be obtained after every 2 sec. from the system. The system reduced the measurement period half by decreasing the sweep period of tunable laser by half, applicable to measure real-time static strain using multi-point FBGs. The system was successfully discriminate the wavelengths between same FBGs and different FBGs, reflected wavelengths of each FBG at different channels independently.

Shinoda *et al.* in 2012 effectively measured static strain in a multiplexing-interference system. An optical method was presented to get rid of multiplexing interferences while using multiple fiber Bragg gratings (FBGs). The experimental setup included circulator passing tunable laser light and interferometer with common-optical path. In each optical fiber, FBGs were placed at equal distances so that the reflected spectra could be acquired at on signal processing. Finally, reflection spectra per required distances were recorded favourably, eliminating interference consequences by simply inserting an offset fiber. The optimised setup was proved to be valuable for long-term monitoring as it accurately recorded spectra's every two seconds from multiple FBGs installed for 24 hours persistently.

Wada *et al*. in 2012 proposed a scheme to achieve distributed lateral loads using long-length fiber Bragg grating (FBG) with optical frequency-domain reflectometry (OFDR). Birefringence was induced by lateral compression at particular areas of long-length FBGs. Nonuniformities of Bragg wavelength were observed because of lateral load in a distributive manner while experimenting. All the results obtained experimentally were good in correspondence to theoretical results, validating this technique to assess manufacturing process and to identify external loads of composite structures. Equal amplitudes of two Bragg peaks, polarization change would be considered to improve the system configuration. The beat cycle was used to measure small uniform lateral loads within the sensing range.

Qiu *et al*. in 2013 designed a polymer optical fiber (POF) operational in few modes to measure temperature and strain variations concurrently. The POF fabrication was based on Teflon technique. Benzyl dimethyl ketal (BDK) was used as photosensitive dopant in the core, to abolish diffraction effect by zero-order. The synthesis of this sensor was grounded on modified Sagnac optical interference method. The synchronous recording of temperature and strain was possible because of the existence of distinct order of propagation modes. The theoretical calculations were accurately backed by experimental results. It was observed that strain measurements were same for all guided modes, whereas temperature measurements showed dependence on order of propagation modes.

Kuse *et al*. in 2013 demonstrated a static fiber Bragg grating (FBG) sensor to analyse the optical response of FBG accurately by using highly sensitive dual-comb spectroscopy which enabled strain measurements with a resolution of 34 nε over a bandwidth of 1-THz. To enhance frequency resolution, a Fabry-Pérot interferometer with a narrow bandwidth could be used and bandwidth improvement was made by reducing the repetition frequency difference to decrease the aliasing effect. Calibration of frequency became impossible on the expense of limitation in measurement time owing to the dual-comb spectroscopy.

Du *et al.* in 2013 exhibited a technique to magnify sensitivity of fiber Bragg grating (FBG) sensors. This improvement in sensitivity was accomplished by degenerated four wave mixing (FWM) which is one kind of all-optical signal processing technologies. This technique demonstrated the successful recording of static strain and temperature. The as measured value of strain sensitivity corresponded to 5.36 pm/με and temperature sensitivity was measured to be 54.09 pm/^{o}c. This method enhanced the sensitivity of FBG by a factor of five, based on 4-order FWM in a non-linear fiber. The post-processing technique, not required pre-processing of sensor head, proved this scheme would be useful in wide range of fiber sensing applications.

Xian *et al*. in 2013 designed and fabricated an economical single FBG sensor based on the power-interrogation method which positively measured temperature and strain variations at the very same time. FBG used in the physical demonstration was linear and chirped, whose reflection spectrum was measured by OSA, at a place where grating ended. The output powers were recorded by a power meter from lights reflected by FBG. Strain and temperature values were recoded concurrently by power-changes at power meter. This sensor proved to be concise, fast and financially favourable as FBG used acted both as a sensor and interrogating element.

Choi *et al*. in 2013 designed a model to measure maximum strain in a beam exposed to various loading conditions developed by characterizing the strain shape functions and participation factors. The maximum strain measurement in a 4 m steel beam subjected to two concentrated loads by the sums of the strains caused by the diverse loadings acting separately. For measurements, seven fiber Bragg gratings (FBG) and nine electric strain gauges (ESGs) were joined on the surface of the bottom flange.

Although, the estimated results from this model were good and directly compared with the strain measured by the ESGs. Besides, the reliance of the areas for the FBG sensors introduced on the beam structure on the selection can be abstained from utilizing the measuring model.

Zhang *et al.* in 2014 effectively measured the bonding layer will cause stress induced birefringence which leads to distortion within surface bonded fiber Bragg gratings (FBGs). Under large strain conditions, serious distortion of the reflection spectrum is caused by mismatch Poisson's ratio of the bonding layer and high elastic modulus. Further, these distortions could limit the available strain measuring range of FBGs. Besides, the stress birefringence magnitude was influenced by material properties and unreasonable geometric parameters within the bonding layer. An appropriate bonding material was chosen to get rid the problem of stress magnitude loss.

Hu *et al.* in 2014 designed and fabricated fiber Bragg gratings (FBGs) at ~1550 nm wavelength by scanning phase mask technique in step-index poly (methyl methacrylate) (PMMA) polymer optical fibers (POFs). This moderation in fabrication was done to achieve enhancement in grating reflectivity and improvement in sensing applications. Reflectivity of 97 % was achieved successfully for 6 mm long FBG by decrease of 12 % in cladding diameter. The absorption of ultraviolet rays caused restrictions up to 25% in the reflectivity. The induced birefringence resulting from transmitted polarized light was calculated to be 7×10^{-6}. The as fabricated sensors could find potential applications in POFs as the calculated results were found to be in correspondence to the silica fiber measurements.

Shi *et al.* in 2014 proposed and developed an effective model of praseodymium-doped fiber (PDF) laser inscribed with fiber Bragg gratings (FBGs) to investigate the performance the PDF in the visible wavelength range. Piezoelectric transducer was used to modulate reflecting spectrum of FBG and to study the influence of feedback, pulse repetition frequency (RPF) and various pulse characteristics. Experimental results proved that this sensor could be better than conventional sensor because of its low threshold and high slope competency. For laser oscillation emplacement, long fiber length, lower output power of green oscillation and large reflectivity of FBG2 for green oscillation were set. The proposed model proved that it was beneficial in various industrial application as it mitigates the effects of large gain factor, obvious multipeak, and spurious pulse.

Chiang *et al.* in 2014 fabricated a notched long-period fiber grating (NLPFG) by using an inductively coupled plasma (ICP) dry etching process. The tunable resonance attenuation loss was exhibited by NLPFG for a particular wavelength. The characterization results of NLPFG showed that with decrease in cladding thickness and increase in number of period (Λ), the redshift of NLPFG wavelength was produced. The wavelength drift followed by change in thickness was -2.801 nm/μm. By increasing the period (Λ), the wavelength drift rate corresponded to the size of the period of 1.466 nm/ μm. Tensile analysis of NLPFG revealed that that the larger the grating period, the longer the wavelength. Moreover,

the results exhibited that etching depth was increasing the transmission loss in the spectra and the variation in transmission loss rate with respect to depth of etching was -0.458 nm/μm.

Shen *et al*. in 2015 presented a technique to study health of hull structures under the environment of fatigue loading and corrosion by using fiber Bragg grating (FBG) strain sensor. Designing of two distinct kinds of FBG strain rosettes was accomplished then they were tested based on the wavelength division multiplexing technology in order to monitor health of hull structure. Strain transfer efficiency was dependent on various factors such as diameter of engulfed material, type of the substrate used and thickness of adhesive layer. To avoid consequences and meets the satisfactory requirements of long term hull health monitoring, re-calibration of FBG sensors were done after being made into strain rosettes and fatigue property test on FBG sensor was conducted respectively. The maximum deviation experienced by wavelength during the process of loading was 18 pm, whereas during the unloading process this deviation corresponded to 10 pm. These perfectly designed FBG strain sensors were stable enough to find practical applications in hull health monitoring. The experimental results proved that the designed FBGs were very stable and would be beneficial to monitor long-term health of hull structures.

Oliveira *et al*. in 2015 fabricated an undoped polymethyl methacrylate (PMMA) fiber with inscribed Bragg gratings in a time record. The fast inscription process was feasible by stable mechanical setup and photo masking technique of PMMA under 248 nm ultraviolet (UV) light. The key factors of the success were the use of low repetition and low influence rate by phase masking technique. The peak reflection of Bragg grating was observed in the infrared region. The Bragg grating peak reflection of 20dB was observed in the infrared region with a bandwidth of 0.16 nm. The inscription method of Bragg grating in few mode (FM) micro structured polymer optical fiber (mPOF) could be used to write gratings in other types of POFs. The model was designed so effectively that the system used to write Bragg grating in silica fiber could have been able to inscribe polymer fiber Bragg gratings. This unique design paving the way its use in both telecommunications and sensor industries intensively.

Chen *et al*. in 2016 proposed improvisation in traditional fiber Bragg gratings (FBGs) by using a л-phase shifted FBG (л-PSFBG) inscribed on polarization maintaining fiber (PMF). Based on the principle of birefringence, this sensor was able to clearly distinguish between strain and temperature variations. Experimental setup consisted of fiber Fabry-Pérot interferometer and $HC^{13}N$ gas cell along with other basic traditional components. The as-fabricated sensor distinctly attained strain resolution of 0.104 με and temperature resolution corresponding to 0.005°C. As the sensor also proved to be stable for long durations, it could be promptly used in geophysical research applications.

Frojdh *et al.* in 2017 fabricated an economical strain sensor using chirped fiber Bragg gratings (CFBG) for measuring strain and temperature variations. The setup system used sensor element made of chirped fiber Bragg gratings of 9.5m length and an optical frequency domain reflectometer (phase-sensitive) was installed as interrogator as optimisation to conventional setups. The prompt localised changes were

successfully detected by as-manufactured sensor. The length of coherence was shortened up to 1 m, own got the fact that the sensor element and reference mirrors could use similar gratings. Thus, the as-manufactured CFBG proved to be a financially beneficial sensor with proficient spatial resolution.

Zhu *et al.* in 2017 demonstrated a technique to measure dynamic strain and temperature simultaneously by employing an Optical Frequency Domain Reflectometer (OFDR), used to measure back reflections from optical fiber networks and components and it has high spatial resolution, based high birefringence PANDA-FBG sensor at sampling rate 800 Hz and spatial resolution of 1mm. They designed an experimental setup in which one FBG sensor was employed as reference parallel with strain sensing FBG in order to decrease the error induced by temperature by subtracting the wavelength shift of stress free FBG with wavelength shift of stress sensing FBG. Although the results were good but not accurate because calibration was done manually.

Pospari *et al* 2017 fabricated a Fabry-Pérot (FP) interferometer sensor based on Fibre Bragg Gratings (FBGs), which investigated stress sensitivity in addition to attenuation effects existing across the path of optical fibre. Polymer optical fiber (POF) was considered over silica optical fiber (SOF), owing to the fact that their Young's modulus was 25 times shorter than the later. These POF based sensors proved to be more sensitive towards stress variations and pressure. The changes in work performance of sensor, in accordance to different optical fiber materials used in manufacturing, when operated in wavelength range of 650 to 1550 nm were discussed. The results concluded that low value of Young's modulus made PMMA FPs best for Shortest cavity lengths, whereas the silica-based sensor's performance was considered best for long cavities, owing to its low fiber loss. The CYTOP exhibited attenuation of 0.02 dB/m in the 1.55 μm wavelength range and higher stress sensitivity in comparison to PMMA and silica-based FPs.

Chein *et al*. in 2017 proposed a scheme to measure simultaneously strain (ε) and temperature (T) with resolution of 0.018 μs/0.0014^{o}C was realised using л-phase shifted fiber Bragg gratings (PSFBG) with double sideband interrogation scheme. The way to enhance the sensing resolution of ε and T was to reduce the measurement error in v_B i.e. frequency difference introduced by mode birefringence. Besides, the narrow resonance could help to achieve higher sensing resolution compared with common fiber Bragg grating (FBG) sensor. Because of the high resolution in concurrent estimation of strain and temperature, the proposed sensor demonstrated great potential in geophysical explores, for example, crustal distortion checking and seismic activity perception.

Pospori *et al*. in 2017 inscribed a polymer optical fiber Bragg gratings (POFBG) in single mode benzyl dimethyl ketal (BDK)-doped poly (methyl methacrylate) (PMMA) optical fiber using krypton fluoride (KrF) pulse laser. The energy density equal to 974 mJ/cm^2 was found to be sufficient for introduction of a refractive record variation of 0.74×10^{-4} in the fiber core. Reflectivity as provided by the POFBG was measured to be 98.4%; suitable for its usage in sensing applications. The outcomes of this work

demonstrated that the reflection control of POFBG increments for a couple of minutes after the UV laser pulse, which showed a triggered photo-polymerization, and photo-crosslinking event. The repetition of process revealed non-stability in the reflection pulse approximately for minutes and the reflected power showed unexpected changes from 15dB to 22 dB of noise level. This method was dominant to inscribe a POFBGs in single mode PMMA and cost effective from industrial point of view.

Xue *et al.* in 2018 proposed a method to precisely and accurate measurement of strain, reinforcement effects on adhesive on object, verified by using numerical method. The material properties of surface-bonded fiber Bragg gratings (FBGs) could distort the strain measurement, lower the measurement accuracy. The numerical and experimental results demonstrated that the strain correction factor could easily affected by recoating material and bonding length. To reduce the effect of material properties of adhesive material and dimensional properties of surface-bonded fiber Bragg gratings, thin as well as short grating length and covered whole area of FBG with adhesive material could enhance the correction precision.

Xing *et al.* in 2018 designed a simple and concise sensor based on PMF (polarization maintaining fiber) of PANDA type and homemade MMF (multimode fiber) with large diameter. This set-up was based on principle of uneven outer diameters. The experimental setup consists of sensing head which was made by sandwiching MMF in between two PMFs. The sensing head was covered by two SMFs (single mode fibers) from both sides. This sensor was able to obtain extinction ratio over 30 dB for spectrum of transmission. The strain variation was measured by recording spectral drifts. In the range of 0 to 2000 με, the dip1 exhibited strain sensitivity of 1.01 pm/με; whereas for dip2 it was calculated to be 1.27 pm/με. And the temperature sensitivities were 49 pm/ °C and 41 pm/ °C for dip1 and dip2, respectively; when input range was 30 to 70 °C. As only ignorable errors of ±4% in strain and ±3% in temperature variation measurements were observed, the as-designed sensor could be used for practical applications in robotics sensing, biological and environment monitoring.

Kumar *et al.* in 2018 proposed a temperature insensitive sensor for calculating strain variations in structures as buildings, dams and poles. As the sensor is based on FBG, whose strain measurements are affected by change in surrounding physical parameters, say temperature. The as-designed sensor was able to terminate temperature sensitivity, as reflected wavelengths were not allowed to overlap. The sensor was found to function accurately at bandwidth of 12 nm. Two FBGs were used in the designing of this sensor and the final value was measured by subtracting shifts in wavelength of both FBGs. This sensor successfully recorded strain variations by abolishing cross sensitivity.

Aldaba *et al.* in 2018 proposed a sensor system capable of measuring multipoint strain and vibrations in temperature concurrently. Rapid phase changes of Fourier transformation were supervised for inquisition of sensing head. The drawbacks faced in multiple interference of frequencies for distinct sensitive components, such as reliance on signal amplitude and requirement of chasing wavelength

spectrum were overpowered through this sensor. The system was made to function in temperature range of 30 to 80 °C with applied strain of 450 με to check multiplexing ability and inquisition method. Basic mathematical algorithms were used to rectify noise or disturbance between measurements.

Wada *et al.* in 2018 proposed a polarisation maintain fiber with contrived Fabry-Perot interferometer for concurrent strain and temperature measurements. Transmission peaks obtained with respect to polarisation were keen and pointed in nature. Two sets depending on distinct temperature and strain shifts, owing to their individual coefficients were recorded precisely. For further betterment, current modulation was injected in laser diode. By this optimisation, measurement time was found to be shortened. In practical exhibition done for 20 με; strain and temperature resolutions were 0.8 με and 0.1 °C. The as-fabricated system recorded amplitude, heating rate and frequency with respective values of 20 με, 0.7 °C/s and 1 Hz concurrently for a particular vibration.

Marques *et al.* in 2018 proposed polymer optical fibers (POFs) based on Fiber Bragg Grating (FBG) engraved with laser. A pulsed laser made from KrF with wavelength 248nm was used. Polymethyl methacrylate (PMMA) and various other polymers were used to fabricate polymer optical fibers. The measurements recorded by this system exhibited 16 times in inscription time as compared to till used UV HeCd lasers. A betterment in reflectivity and bandwidth was obtained than previously used systems. Thus, the as-presented system demonstrated a little drift in central wavelength (CWL), implying high stability even after 40 days.

Lu *et al.* in 2018 designed an easy to make and concise few-mode fiber-based sensor system which was able to record variations in strain and temperature at the same time. the specifications of the FMF were set in a way that only LP_{01} and LP_{02} modes were able to sustain. The concurrent measurements were based on principle that the peaks on extreme sides of CWL (critical wavelength) exhibited distinct drifts in opposing direction to each other. The as-proposed theoretical results for as-fabricated sensor system were found to be in good agreement with experimental measurements. Being economical, concise in design and well accurate in results this system could be used in many practical applications for structural health monitoring.

2.3 OBJECTIVES

1. Design and simulate optical sensor to enhance sensitivity for structural health monitoring.
2. Investigate FBG sensor to monitor strain and temperature.
3. To analyze the effect of strain on metal rods using FBG sensor.

CHAPTER-3

DESIGN AND SIMULATE OPTICAL SENSOR TO ENHANCE SENSTIVITY

3.1 INTRODUCTION

There has been extensive enthusiasm for creating techniques which empower optical fibers to quantify strain and temperature at the same time [72-73]. These optical fiber sensors are normally made by distinguishing two physical parameters which have diverse sensitivities to temperature and strain. Fiber Bragg gratings (FBGs) have been of awesome enthusiasm for optical detecting innovation as of late on the grounds that they are cost-effective, small, simple to fabricate, and their optical spectra have great linear responses as for varieties of temperature and strain [74]. Numerous methods in view of FBGs have been accounted for concurrent strain and temperature separation, for example, utilizing two superimposed FBGs, two resolvable wavelengths in a tilted FBG [75], two FBGs of different diameters or with diverse composition written in fibers [76], and a single FBG of different refractive index between fibers across a splice point [77-80] or between fibers with various levels of doping components. Then again, the estimation from an FBG might be joined with that of an alternate detecting method, for example, utilizing cross hybrid FBG/long period fiber grinding (LPG), superstructure FBG, an inspected FBG joined with an LPG, and an FBG joined with a polarization-keeping up fiber loop mirror [81-85]. Numerous different strategies can likewise be found in the review article on this subject.

On the other hand, all the fiber Bragg grating sensors based on different refractive index have increasingly aroused research interests in the last decade because of many advantages like they are highly sensitive, high immunity to electromagnetic interference (EMI), high spatial resolution and stability [86-89].

In monitoring structural health, vibration and environmental parameters, fiber optic sensors are extensively used. Among all the optic sensors, fiber Bragg grating sensors are the best for this purpose because they have high sensitivity, stable, compact in size, able to withstand with harsh conditions and moreover immune to electromagnetic interferences. Fiber Bragg grating sensors are specifically used to measure parameters like strain, pressure, temperature, and vibration [90-94].

3.1.1 Principle of Operation

The Bragg wavelength (λ_B) is defined by the grating period of different refractive index (Λ) and the index of refraction of core ($n_{eff.}$).

$$\lambda_B = 2 \times n_{eff} \times \Lambda \tag{3.1}$$

The unique characteristics of fiber Bragg grating makes it to perform as a sensor. For instance, when the fiber is compressed or stretched, the FBG will measure strain. Basically, this happens due to

deformation of optical fiber which further leads to change in period of grating and consequently, of Bragg wavelength. Apart from that there is also a role of photoelastic effect which cause variation of core index of refraction [95-99]

3.2 DESIGN A HIGHLY SENSITIVE FIBER BRAGG GRATING SENSOR

For optimization purposes, a schematic diagram of fiber Bragg grating sensor is shown in figure. It consists of two cylinders, where inner cylinder acts as core and outer cylinder acts as cladding. The grating length and number of periods is calculated by:

$$L = 2 \times N \times P \tag{3.2}$$

where,

N = number of grating periods,

P = grating period.

In general, an fiber Bragg grating (FBG) is a periodic change of refractive index across the length of fiber which is made by alter the core index of refraction by optical absorption of UV light in a single mode optical fiber. By increasing the number of gratings, the length of grating increased. Further increments in grating length may have an insignificant impact on spectrum.

The proposed fiber Bragg grating (FBG) sensor is a three-dimensional (3D) model. The geometry for the fiber Bragg grating sensor consists of two cylinders: core and cladding. Here, the refractive index of first cylinder which is representing core is taken as 1.4457. The gratings are inscribed within the core of fiber with a material of refractive index of 1.4467. In general, the difference between refractive index of gratings and refractive index of core is in order of 10^{-3}, known as amplitude of induced refractive index (d_n). The refractive index of other cylinder represented cladding is taken as 1.4357 and the difference between refractive index of core and refractive index of cladding is in order of 10^{-2}. A specific set of parameters are used to define its geometry and their expressions are listed below with description:

Table 3.1 List of parameters to design and simulation of sensor

NAME	EXPRESSION	VALUE	DESCRIPTION
n_core	1.4457	1.4457	Core Refractive Index
n_cladd	1.4357	1.4357	Cladding Refractive Index
n_gratings	1.4467	1.4467	Gratings Refractive Index

Dn	10^{-3}	0.001	Amplitude of Induced Refractive Index Perturbation
N	3000	3000	Number of Periods
P	500[nm]	5E-7 m	Grating Period
L	0.05[cm]	5E-4 m	Fiber length
n_eff.	n_core+(dn*cos((2*pi*L)/(P)))	1.4467	Effective Refractive Index
lambda	2*n_eff.*P	1.55E-6 m	Incident Light Wavelength
f_o	c_const/lambda	1.9341E14 1/s	Frequency of Light
r_core	4.6[µm]	4.5E-6 m	Core Radius
r_cladd	62.5[µm]	6.25E-5 m	Cladding Radius

For designing an fiber Bragg grating sensor, an inner cylinder i.e. core of sensor is designed with a radius of 4.6 µm and length of 0.05 cm. The graphical representation of core is shown in figure 3.1.

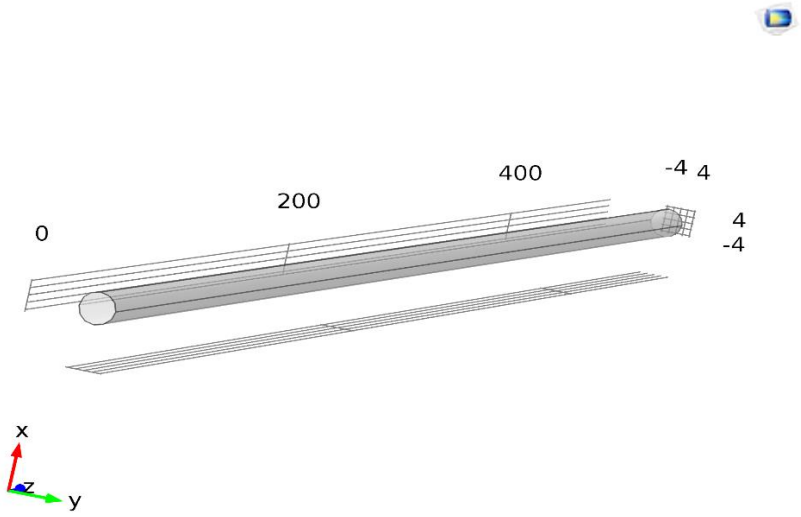

Figure 3.1 Core of fiber Bragg grating (FBG) sensor.

Secondly, Bragg gratings are inscribed inside the fiber core with a radius of 4.6 µm and having grating period of 500 nm. To make the sensor very sensitive, the number of periods is considered as 3000 as shown in figure 3.2.

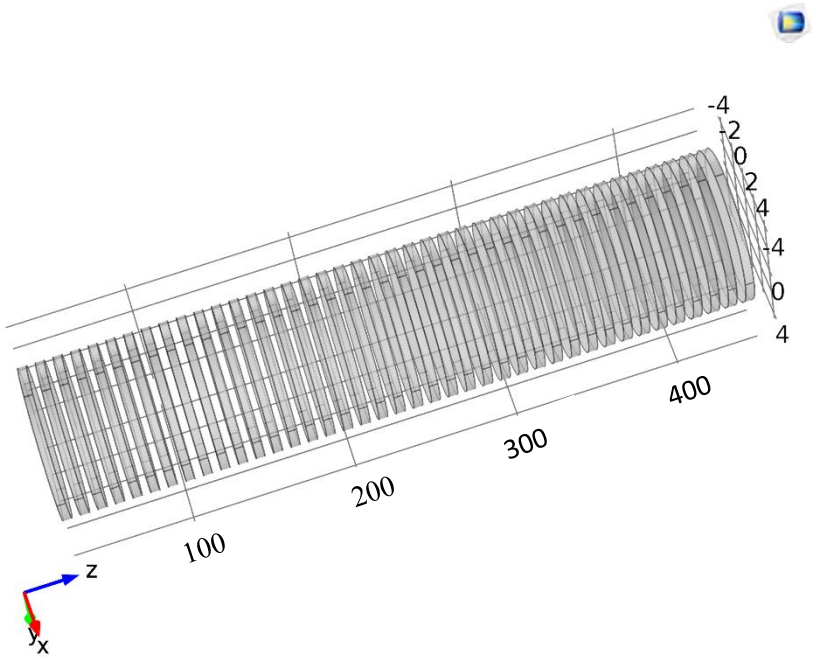

Figure 3.2 Bragg gratings of fiber bragg grating sensor.

Next step, is to design an outer cylinder i.e. cladding with a length of 0.05 cm and having radius of 62.5 µm. The graphical representation of cladding is shown in figure 3.3.

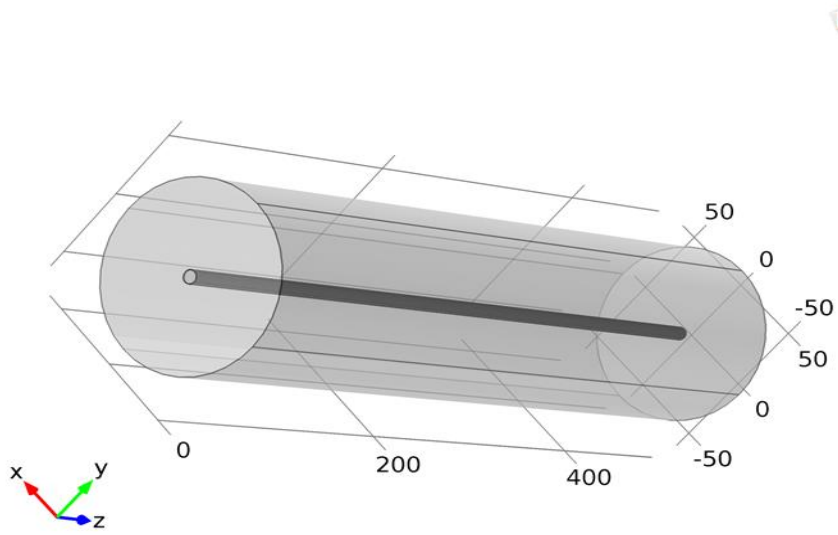

Figure 3.3 Cladding of fiber bragg grating sensor

Further, from the physics interface, the electromagnetic waves, frequency domain interface (ewfd) is used to solve for time harmonic electromagnetic field distributions. For the physics interface, the mesh element size should be limited to a fraction of wavelength. The scaling of available memory and the wavelength is done by a possible simulated size of domain. The 3D wave equation for this domain is given by:

$$\nabla \times (\nabla \times E) - K_o^2 \varepsilon_r E = 0 \tag{3.3}$$

The eigen values calculated by COMSOL are in the form:

$$\lambda = -i\beta - \delta \tag{3.4}$$

$$\varepsilon_r = (n - ik)^2 \tag{3.5}$$

$$k_0 = w\sqrt{\varepsilon_o \mu_o} = \frac{w}{c_o} \tag{3.6}$$

where,

E = incident electrical field

δ = real part of solution responsible for damping

β = Eigen frequency

n = refractive index (real part)

k = imaginary part of refractive index

k_0 = wave number of free space

μ_o = permeability of free space

c_o = speed of light in vacuum

A scattering boundary conditions are used. The boundary transparency for both incident light and scattering light is made by the scattering boundary. The incident wave i.e. electric light field has a propagation wave towards z-direction, in (x, y, z) the incident wave is set to be (-1, 1, 0). For this boundary the model equation is given by:

$$\nabla \times (\nabla \times E) - ikn \times (E \times n) = -n (E_o \times (ik (n - k_{air}))) e^{ik.kair} . r \tag{3.7}$$

$$E_{sc} = E_{sc} e^{-ik (n.r)} \tag{3.8}$$

$$E_{sc} = E_{sc} e^{-ik (n.r)} + E_0 e^{-iK (kair. r)} \tag{3.9}$$

where, k is directional vector of wave, E is the incident plane wave and K is wave number.

Port conditions are chosen from physics toolbar to excite the model with electromegnetic wave at input port but wave excitation is off at output port. The port 1 and port 2 are shown in figure 3.4.

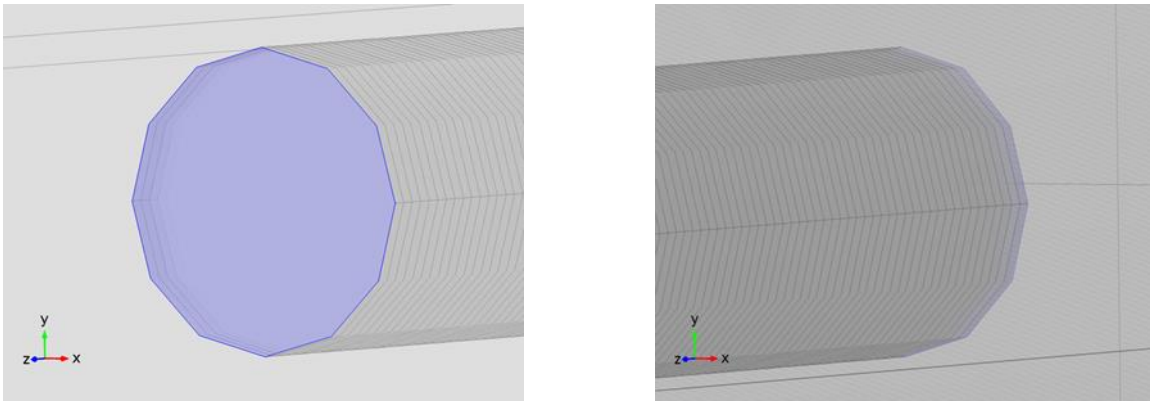

(a) (b)

Figure 3.4 (a) Input port 1, (b) Output port 2

In order to avoid large computation time to solve while simulation process, a perfect meshing should be required. This can help to reduce the memory requirements and provide accurate information data. Identifying the best-suited mesh for your specific model often comprises of choosing the correct element type and size. Here, tetrahedra element technique is used. For cladding the maximum element size is 27 μm and minimum element size is 2 μm. For core and gratings, the maximum element size is 300 nm.

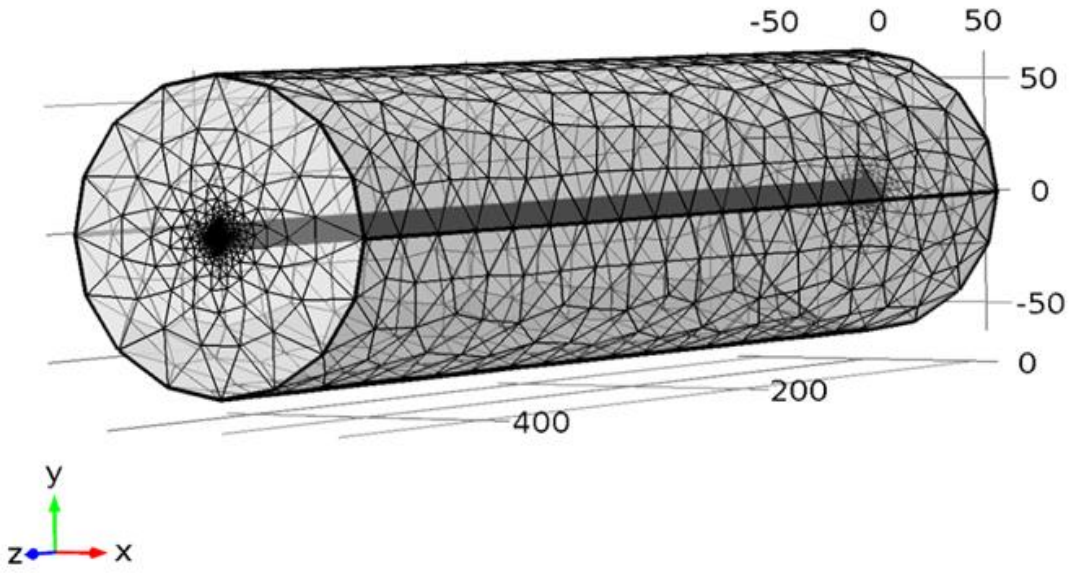

Figure 3.5 Meshing of fiber bragg grating

3.2.1 Results and Discussions

The response of highly grated FBG sensor is promising as it is capable of measuring strain and temperature concurrently with a high accuracy. The Bragg gratings are acting as a spectral filter that reflecting specific wavelengths of light near Bragg resonance wavelength and the remaining spectrum of optical signal is being released. FBGs used in sensors are mostly depends on the spectrum analysis of wavelengths those are reflected back in small amount at each periodic refraction change; combined coherently to one large reflection at a specific wavelength. The following graphs are the results after simulation of designed highly sensitive fiber Bragg grating sensor at 1550 nm.

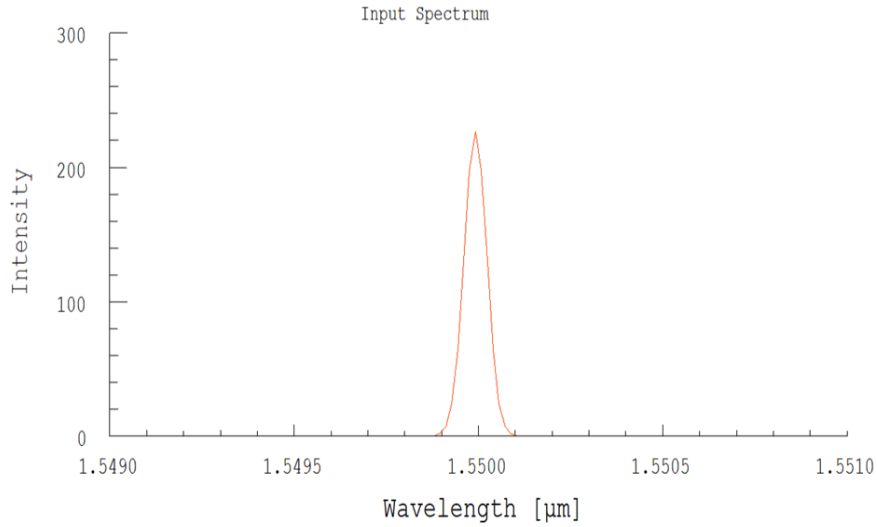

Figure 3.6 Input spectrum

Although, most of the light wave couples across the Bragg gratings when fields are transmitted through fiber Bragg gratings optic fiber sensor as observed in following transmission power spectrum figure below:

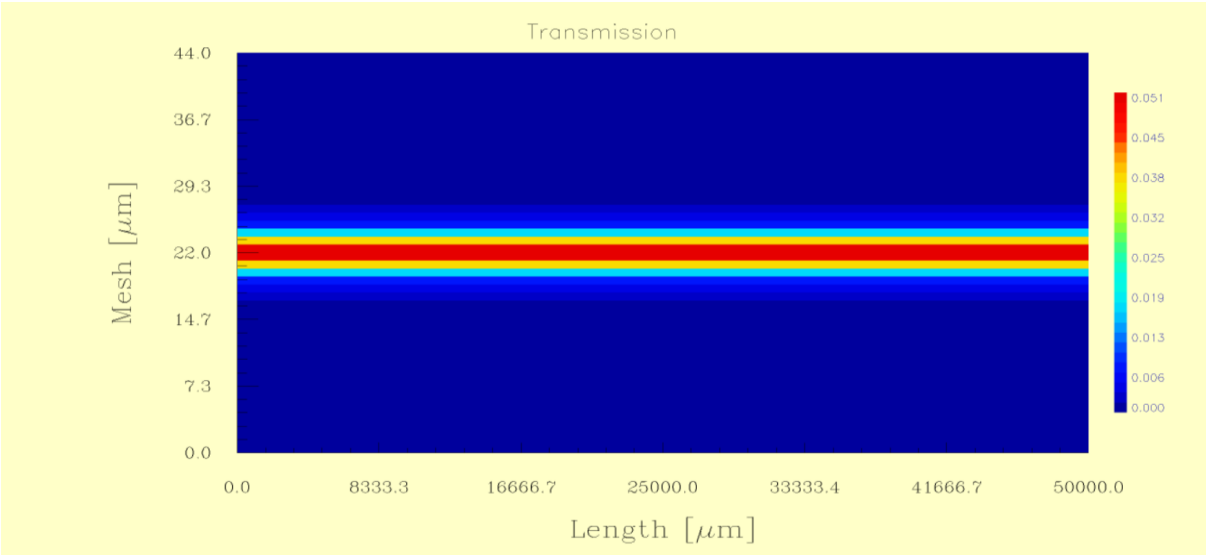

Figure 3.7 Transmission power spectrum

The following results depict that the transmission curve for fiber Bragg gratings optic fiber sensor has a dip in the range of 1.5505 µm to 1.5510 µm and an improvement is made in shift by increasing number of grating periods inside core of optical fiber. The transmittivity/reflectivity vs wavelength graphs are shown in figure 3.8.

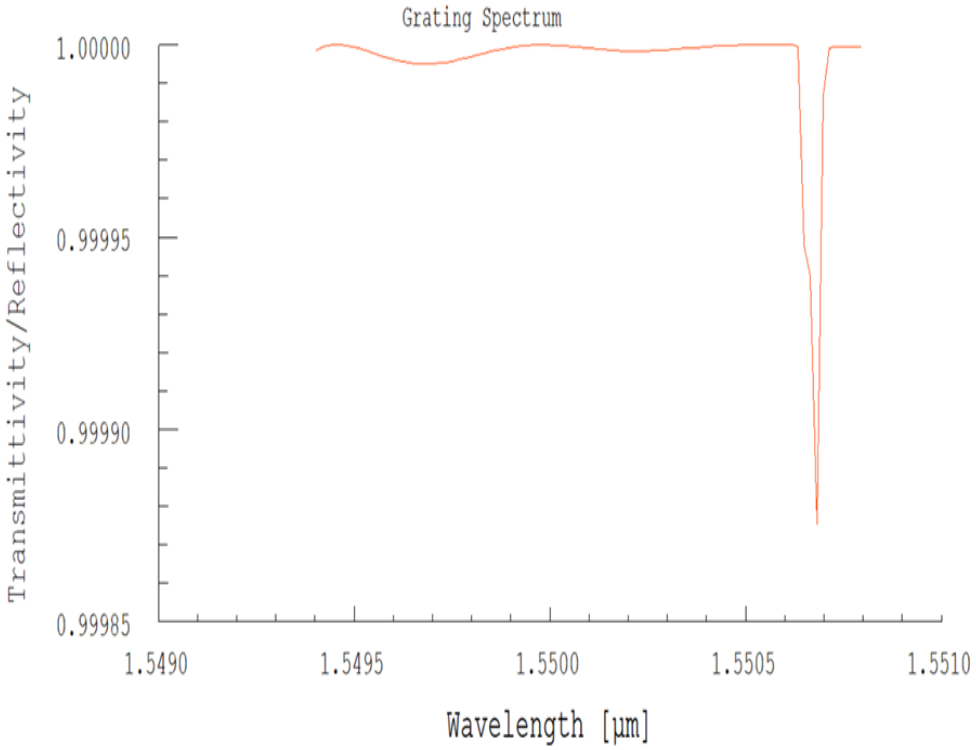

(a)

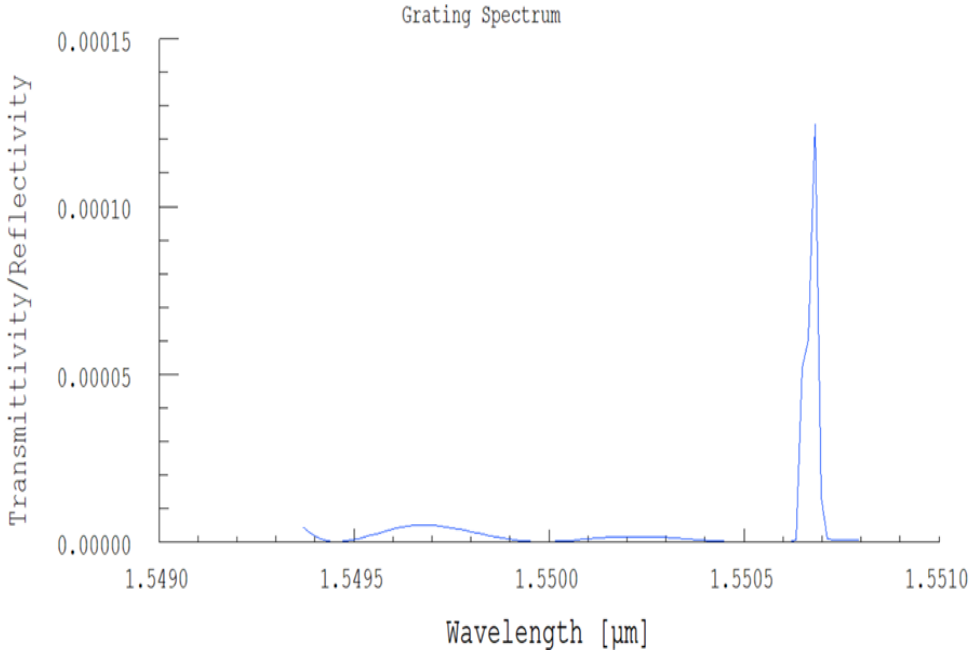

(b)

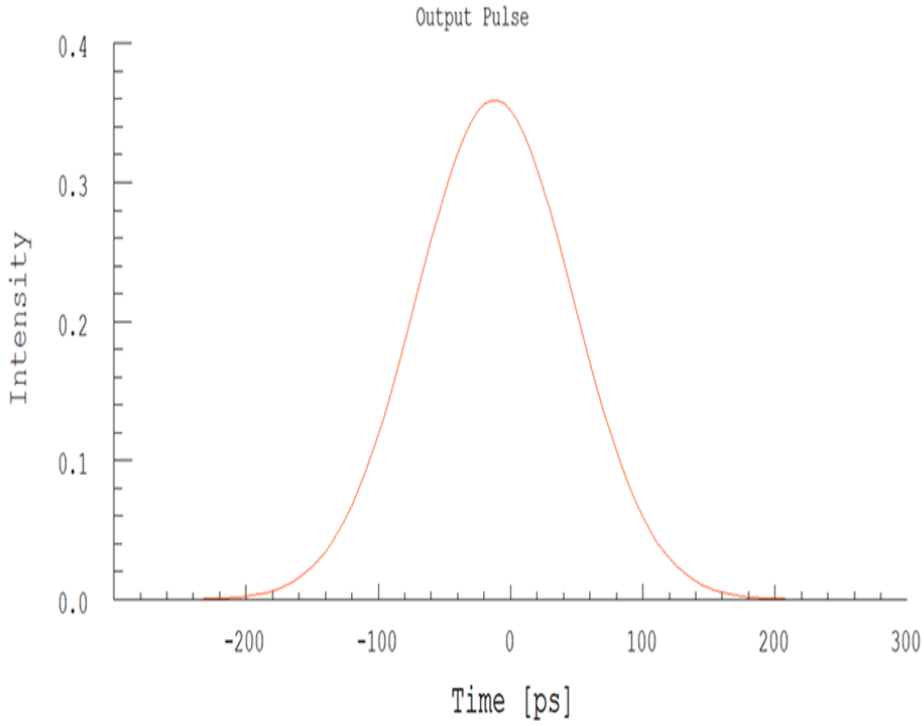

(c)

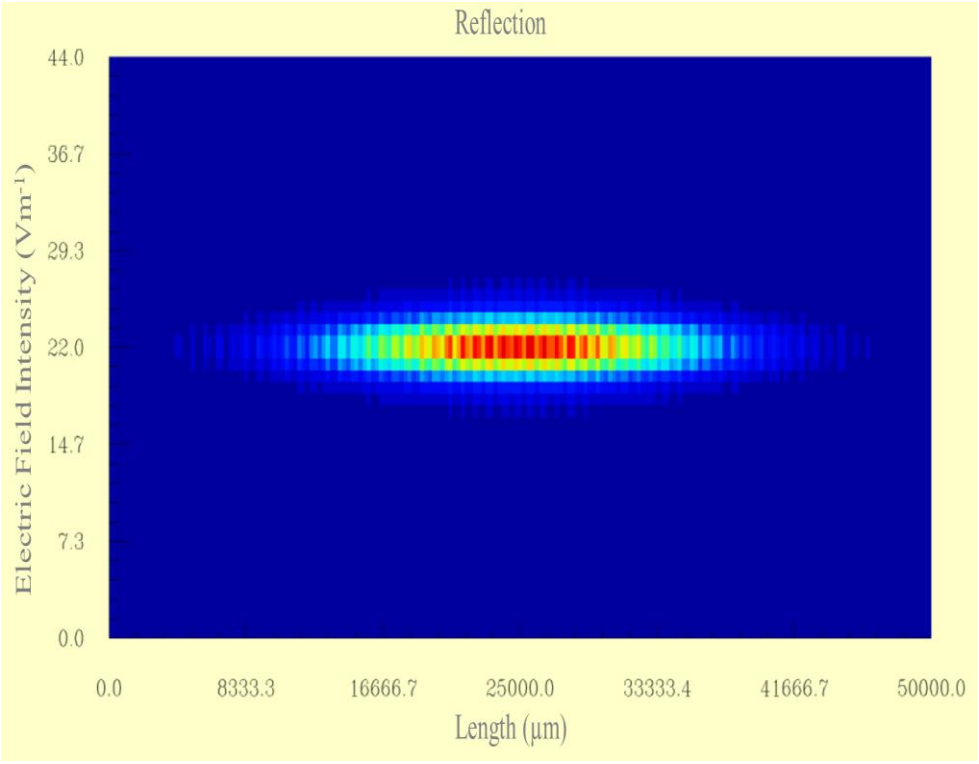

(d)

Figure 3.8 (a) Transmittivity grating spectrum, (b) Reflection power spectrum (c) Output pulse, (d) Grating profile.

3.3 DESIGNED FBG SENSOR TO MONITOR STRAIN AND TEMPERATURE

In monitoring structural health, vibration and environmental parameters, fiber optic sensors are extensively used. Among all the optic sensors, fiber Bragg grating sensors are the best for this purpose because they have high sensitivity, stable, compact in size, able to withstand with harsh conditions and moreover immune to electromagnetic interferences. Fiber Bragg grating sensors are specifically used to measure parameters like strain, pressure, temperature, and vibration.

The fiber Bragg grating sensors provides information in wavelength encoded form, i.e. when strain is applied to the fiber Bragg gratings, it causes shift in the Bragg wavelength (λ_B) of the FBG spectral. In order to recover the output data from the encoded wavelength, a system is required which must be able to detect changes in wavelength accurately. For this purpose, an optical spectrum analyzer is used. On the other hand, an interrogation system is required to map encoded output data into power measurement. To study and analyse the effect of dynamic strain on a particular temperature, simulation has been performed.

The results after simulation clearly demonstrated that the applied strain of ε=150 at a temperature of 25ºC on fiber Bragg gratings for a single mode fiber (SMF) causes a shift in Bragg wavelength (λ_B) of 1.5500 nm to 1.55015 nm. The shift in peak wavelength of FBGs sensor spectral response is shown in figure 3.9.

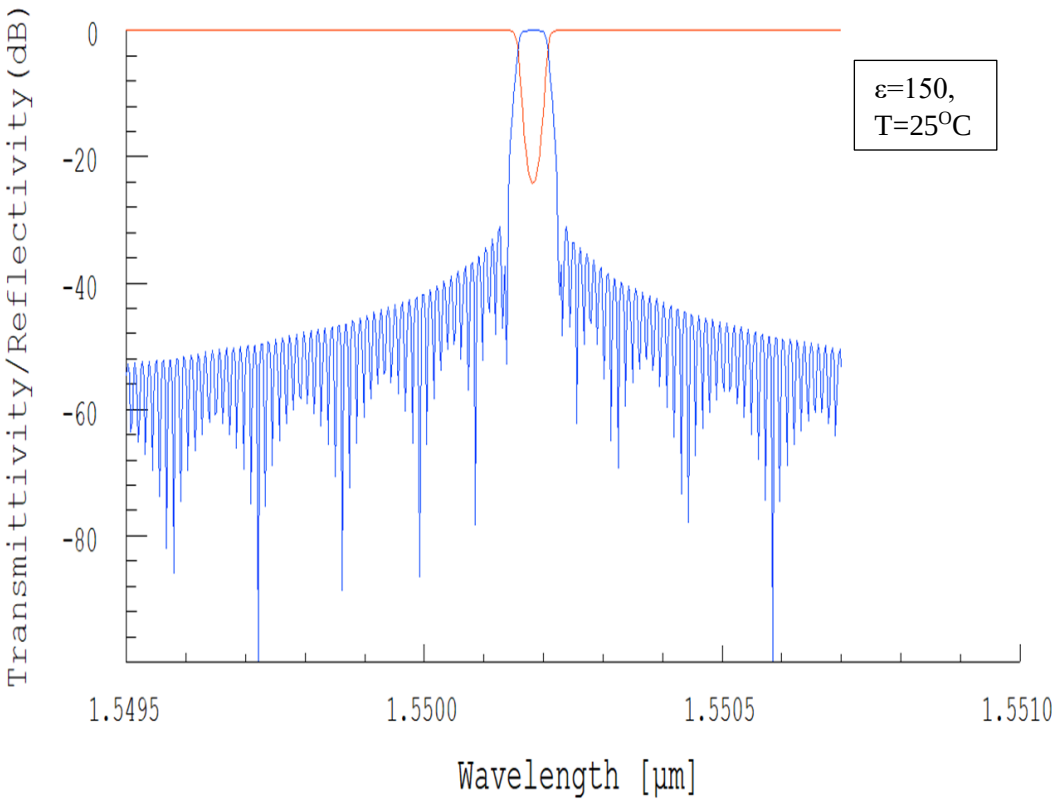

Figure 3.9 Power spectrum: wavelength vs transmittivity/reflectivity

Here, the simulation results revealed that the effect of dynamic strain i.e. ε=250 on the peak wavelength of FBGs sensor spectral response i.e. 1.55 nm when a linear temperature is applied within the range of 0ºC – 50ºC. The graphs depicted that the reflectivity wavelength is wide i.e. a broad shaped pulse has been observed.

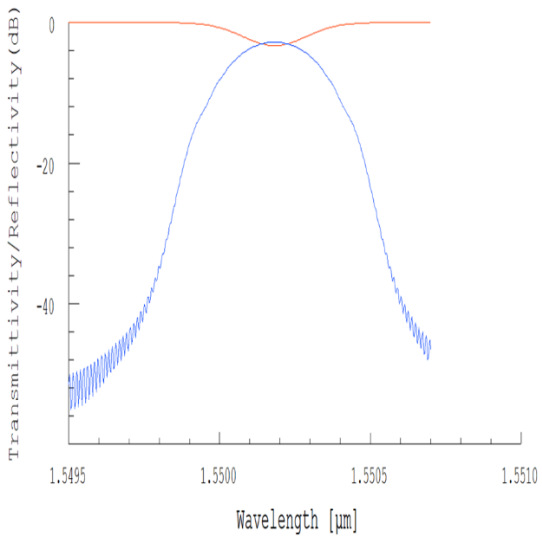

(a)

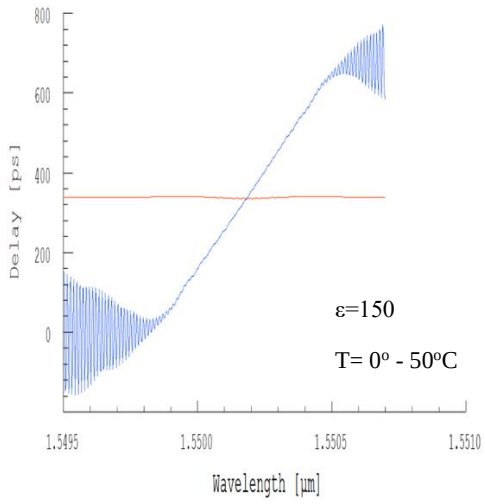

(b)

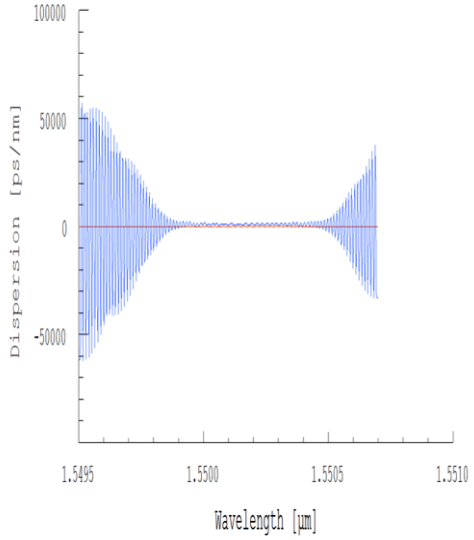

(c)

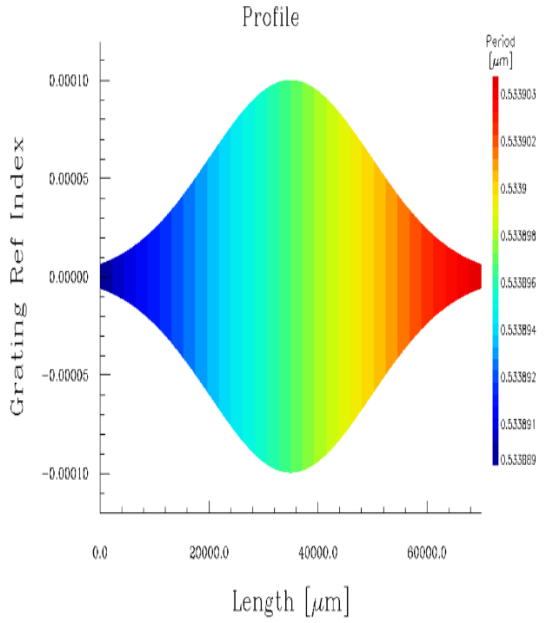

(d)

Figure 3.10 (a) Power spectrum, transmittivity/reflectivity vs wavelength when ε=150 and T is linear (0 ºC – 50 ºC), (b) Transmission delay vs wavelength, (c) Dispersion vs wavelength, (d) Grating profile.

A specific set of parameters is used to calculate their expressions are listed below with values:

Table 3.2 Grating Definition

S.No.	Name	Value
1	Grating shape	Sine
2	Average index	Uniform
3	Period chirp	No chirp
4	Apodization	Gaussian
5	Grating length (L) (μm)	70000
6	Index modulation (dn/H)	0.0001
7	Shift	0
8	No. of segments	1000
9	Period (P) (μm)	0.53381599
10	Taper's parameter	0.5
11	Index change	0

The list of sensor parameters used to calculate power spectrum, delay and dispersion are given below:

Table 3.3 Sensor parameters

S. NO.	Name	Value
1	Static-optic parameters: Photoelastic coefficient	p_{11}=0.121 p_{12}=0.27
2	Poisson's ratio	0.17
3	Thermo-optic parameters: Thermal expansion coefficient Thermal-optic coefficient	 5.5E-007 8.3E-006
4	Temperature (linear)	0^oC – 50^oC

The simulation operation is performed to observe and analyse the effect of strain and temperature on the transmitted wavelength propagating through optical fiber. The results demonstrated that different load values produce unique shift in peak transmitted/reflected wavelength of FBG spectral response at

a particular temperature. The results shown in Fig.5 shows effect of strain at a constant temperature (T = 25 ℃). For this simulation, various amounts of load (150, 200, 250 and 300) are applied

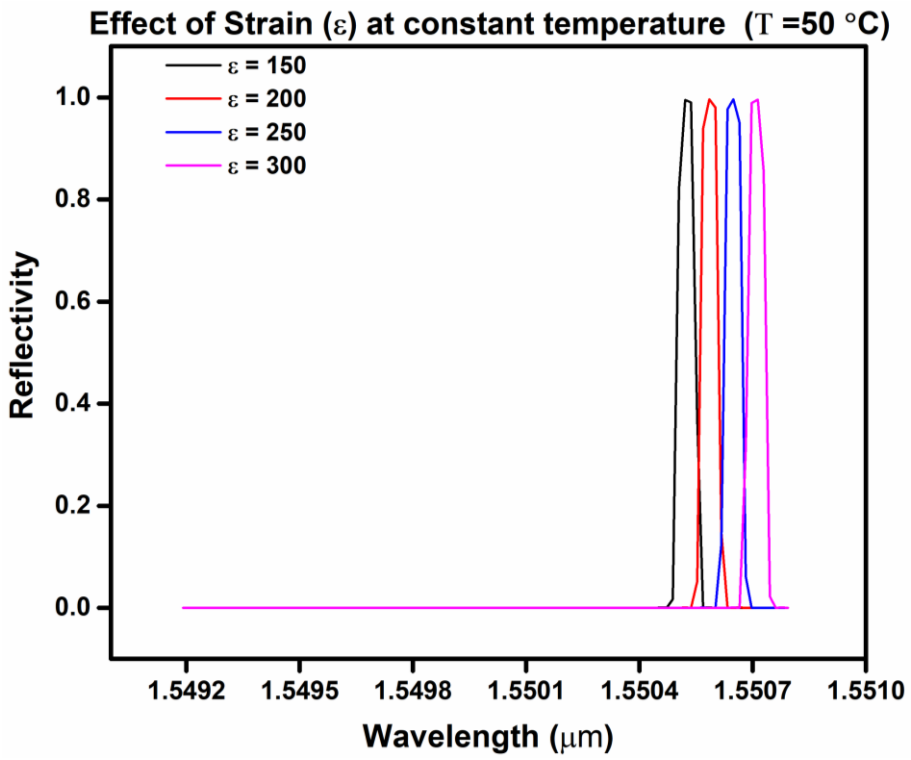

Figure 3.11: Effect of strain on wavelength

Figure 4 shows the shift in bragg wavelength as per introduction of different strain values at a particular temperature (T=50 ℃). The strain applied of 1 [pm/μm], causes 0.002 nm shift in bragg wavelength ($\Delta\lambda_B$). To check the performance of fiber bragg grating sensor, the strain values of amount of 150, 200, 250 and 300 [pm/μm] are applied.

Table 3.4 Values of strain at constant temperature

Temperature (℃)	Strain (ε)	Wavelength shift (nm)
T = 50	150	0.521
	200	0.585
	250	0.649
	300	0.714

As per the plots depicted in Fig.4, a uniform shift (~0.064 nm) has been observed in the peak wavelength of fiber bragg grating sensor spectrum, when strain applied is changed linearly (50 [pm/μm] per simulation). The table 3 shows particular wavelength shift for each value of strain applied at temperature (T=50 ℃).

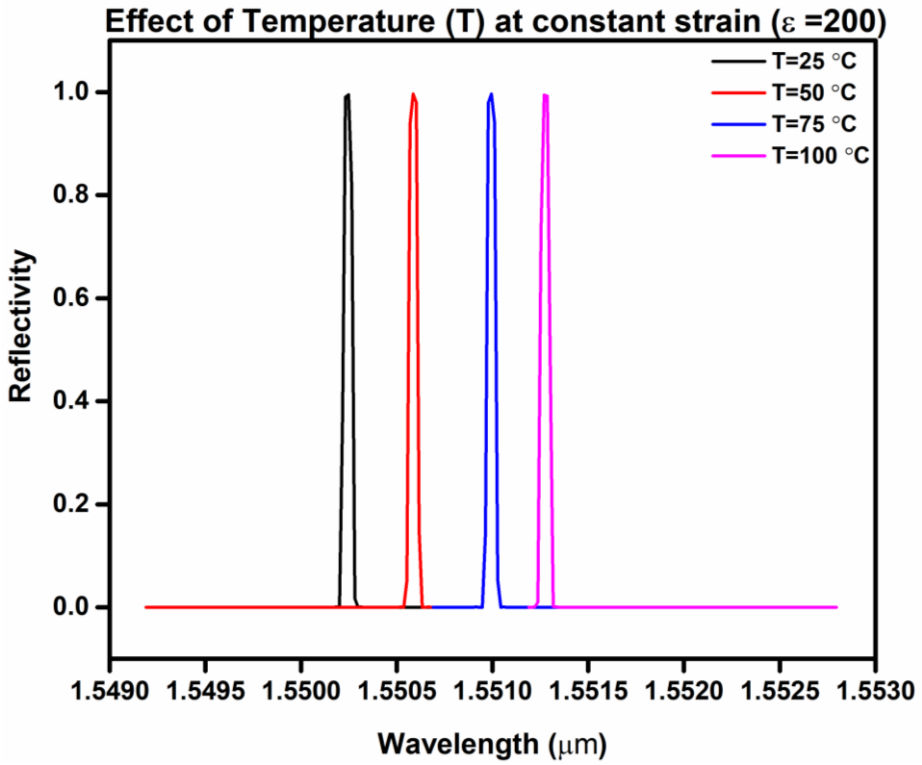

Figure 3.12: Effect of temperature on wavelength

The shift in bragg wavelength of fiber bragg grating sensor as per the effect of temperature has been plotted in Fig.5. The value of temperature is varied independently from 25 ℃ to 100 ℃ through linear steps of 25 ℃, whereas the value of strain (ε) is kept constant at 200 pm/μm. The results indicate the linear relationship between temperature applied and wavelength shift. A uniform shift of ~0.347 nm is obtained corresponding to every change in temperature.

Table 3.5 Values of temperature at constant strain

Strain (ε)	**Temperature (℃)**	**Wavelength shift (nm)**
ε = 200	**25**	**0.238**
	50	**0.585**
	75	**0.930**
	100	**1.277**

The per degree rise in temperature in accordance to wavelength shift is calculated to be 17 pm/℃, indicating the enhanced sensitivity of as-proposed fiber bragg grating sensor. The table 4 refers to shift in wavelength with per step increase in temperature.

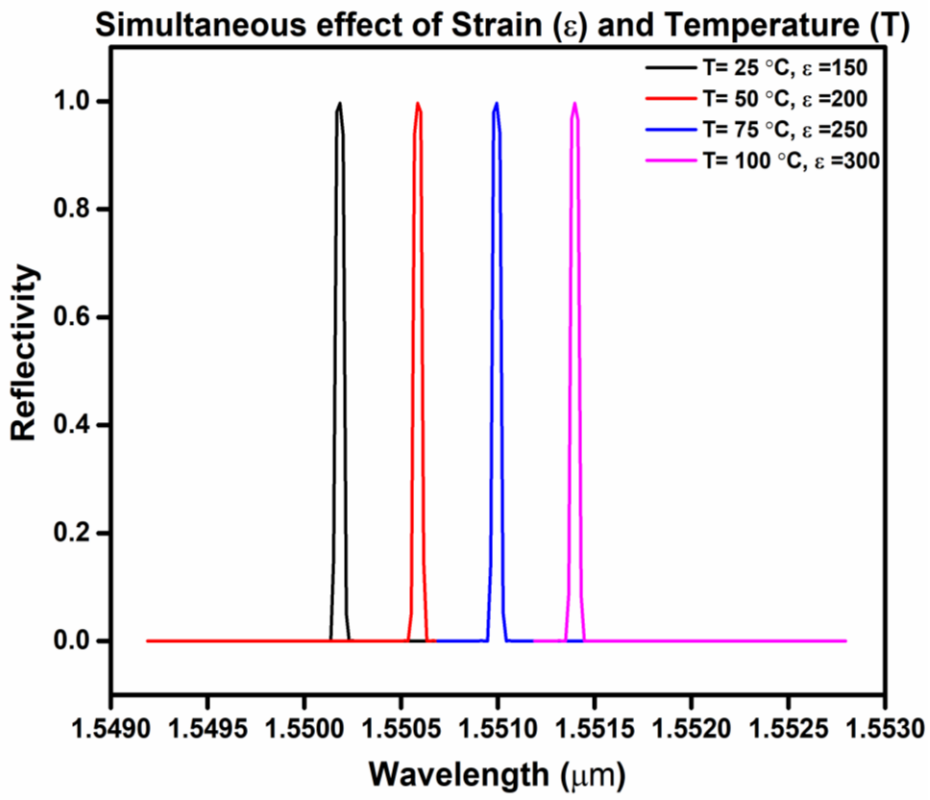

Figure 3.13 Effect of strain and temperature on wavelength

The concurrent study of temperature (T) and strain (ε) has been observed via increasing these both linearly at the same time. The rise in temperature from 25 to 100 ℃ through steps of 25 ℃ and upsurge in strain from 150 to 300 pm/μm through uniform steps of 50 pm/μm are taken under consideration. It is found that bragg wavelength is directly proportional to change in temperature (T) and strain (ε) taken simultaneously, as shown in Fig.6. As per the linear change in these values, a uniform shift of ~0.406 nm in bragg wavelength is achieved. Correspondingly, the table 5 depicts the wavelength shift for each value of strain and temperature taken for simulation.

Table 3.6 Values of strain and temperature

Temperature (℃)	**Strain (ε)**	**Wavelength shift (nm)**
25	**150**	**0.182**
50	**200**	**0.585**
75	**250**	**0.994**
100	**300**	**1.404**

The specific set of parameters required to calculate these results are listed below:

Table 3.7 Single fiber calculation

S.No.	Name	Value
1	Wavelength	1.55[μm]
2	Steps	100
3	Time span [ps]	500
4	Length [km]	100
5	Chromatic dispersion [ps/nm*km]	18
6	Intensity FWHM [ps]	50

3.4 CONCLUSION

We have proposed a grating-based strain sensor for monitoring the health of massive structures. It is concluded that with increase in number of gratings in fiber Bragg gratings sensor, the shift in peak wavelength of FBG spectrum wavelength has been achieved desirably, with respect to independently applied strain and temperature. The same simulation is performed to efficiently record concurrent effect of strain and temperature. All these cases show linear shift in bragg wavelength as per uniform change in input parameters. These results reveal enhanced sensitivity of FBG sensor for strain and temperature corresponding to 2 pm/μstrain and 17 pm/°C, respectively. Hence, the simulation results are very useful in the designing of FBG strain sensor which further can be used to measure strain at huge buildings, flyovers, pillars in manufactory and some infrastructures. Moreover, considering the high temperature sensitivity this as-proposed sensor could be well exploited in the bakeries, steel and oil industries as well.

CHAPTER-4

MEASUREMENT OF STRAIN WITH FIBER BRAGG GRATING SENSOR FOR STRUCTURAL HEALTH MONITORING

4.1 INTRODUCTION

In structural engineering, structural health monitoring is a great topic of interest, due to aging of built massive structures and increasing the use of innovative techniques for structural networks and for construction materials [100]. Although various techniques have been developed for sensing purpose in structural health monitoring systems but fiber optic sensors, especially fiber Bragg grating sensors have become very popular and demanding due to their advantages over other types of fiber optic sensors.

For the purpose of in situ, regular (routine) or continuous analysis and measurement of key structural and environmental factors under operating states, admonition of incidents at an early stage or of impending abnormal states, as well as providing maintenance and rehabilitation consultation, structural health monitoring is required [101-105].

A monitoring system comprises of three fundamental elements: a detecting system, an information processing framework and a health evaluation framework. Sensors that are able to detect the transmitted electrical signal have traditionally been used for structural health monitoring, but in the past decade the use of fiber optic sensors has pulled a great deal of consideration in development and research. The prime reason for this attention is the falling costs of fiber optic sensors over the use of conventional sensors. These advantages are mainly related to their small size, flexibility, immunity to electromagnetic interference, multiplexity, high sensitivity and embeddability [106]. Fiber optic sensors are able to detect variations in characteristics of light travelling through the cable of optical fiber.

Usually, the fiber comprises of three layers: the core, inner cladding and outer cladding. In detail, the core is thin glass fiber and is main medium for the propagation of light inside fiber, the cladding limits the propagating of wave inside the fiber and the outer jacket provides the fiber a great mechanical strength and protects it from moisture absorption and damage. Although, there are three diverse fiber optical sensor technologies available (point, distributed sensors and long gauge) but the most commonly used system is the fiber Bragg grating point sensor.

There are some points which must be taken into consideration while installation of fiber Bragg grating sensors. These sensors must not be installed bare in a structure as they are very fragile and the rigid environment of building structures and construction site would affect their behaviour and durability. Therefore, various packaging or encapsulation techniques have been developed in order to protect them. Usually, the strain esteems recorded by fiber Bragg grating sensor are expected to be the real strains in the host structure, yet this isn't generally the case. In the regular case of sensors that are first installed in a material or settled to a plate and afterward glued to the surface of the host structure, an inconsistency

seems identified with the thickness of the inserting material or settling plate and the thickness and mechanical properties of the glue.

4.2 PRINCIPLE OF OPERATION

An FBG is a reflector, worked in a short fragment of the centre of an optical fiber by presenting the fiber to an extreme UV light [91,92,93]. This presentation makes periodic variation in the index of refraction of the fiber core, called Bragg gratings, and makes the FBG (1) reflect just specific narrowband wavelengths of light, known as Bragg wavelengths, and (2) transmit all others [94]. The Bragg wavelength condition is given by Eq. (1),

$$\lambda_B = 2n_{eff}\Lambda \tag{4.1}$$

where,

λ_B = wavelength of the FBG,

n_{eff} = successful refractive list of the fiber centre; and

Λ = Bragg grinding period or separation between two back to back modifications of the fiber centre.

The external perturbations like strains and temperature variations induce alteration in the Bragg grating period. The modification in Bragg grating also induces a shift in Bragg wavelength. This shift in wavelength is given by equation (2) [95], when only the dominant effects of strain and temperature on an FBG are taken and cross-sensitivities of higher order are neglected.

$$\frac{\Delta\lambda_B}{\lambda_B} = K_\varepsilon \Delta\varepsilon + K_T \Delta T \tag{4.2}$$

In the above equation, the K_ε and K_T are the wavelength sensitivity coefficients to strain and temperature for an fiber Bragg grating sensor whose values are given by:

$$K_\varepsilon = [1 - 0,5n_{eff}(p_{12} - \nu(p_{11} - p_{12}))]\lambda_B \tag{4.3}$$

$$K_T = [1 + \xi]\lambda \tag{4.4}$$

where, p_{11} and p_{12} are fiber optic strain tensor components and ν stands for the Poisson's ratio of fiber, ξ is the thermo-optic coefficient of fiber and n_{eff} i refractive index of fiber [95-.

K_ε and K_T coefficient values are obtained from the experiment, K_T coefficient value is dependent on the host structural material. Once K_T and K_ε are calculated, it is possible to get the values of increments in temperature and strain corresponding to a central wavelength shift by using equations (4.5) and (4.6).

$$\Delta\varepsilon = \frac{1}{K_{\varepsilon}}\left(\frac{\Delta\lambda_{B1}}{\lambda_{B1}}\right) - \frac{K_{T1}}{K_{\varepsilon 1}K_{\varepsilon 2}}\left(\frac{\Delta\lambda_{B2}}{\lambda_{B2}}\right) \tag{4.5}$$

$$\Delta T = \frac{1}{K_{T2}}\left(\frac{\Delta\lambda_{B2}}{\lambda_{B2}}\right) \tag{4.6}$$

For this particular fiber Bragg grating sensor, $K_{\varepsilon 1}$ is equal to 1.15 pm/με whereas the value of K_{T1} is equal to 20.5 pm/^{o}C because host structure is made of steel. K_{T2} value depends on the type of sensor used to measure temperature variations and its value is equal to 8 pm/^{o}C for this system.

4.3 EXPERIMENTAL SETUP

The FBG strain sensor comprises of an FBG guarded by layers of composite material made of glass fiber polyester pitch with a weight of 300 g/m2. The sensor framework is around 0.5 cm long, 10 mm wide and 0.6 mm thick, and is settled to the host metal or solid structure with a thin layer of a glue whose specialized determinations are nitty gritty in Table 1.

Table 4.1 Adhesive specifications

Properties	**Units**	**Value**
Coefficients of thermal expansion	$^{o}C^{-1}$	$3.5 – 4 \times 10^{-6}$
Thermal conductivity	K_{cal}	0.16 (between 0 and 40 ^{o}C)
Young's modulus after hardening	N/mm^2	2000
Resistance	Ω	$>10^{14}$
Temperature limits for strain measurement	^{o}C	-200……. +60

The following details should always be kept in mind:

- The FBG is put on one of the bundling surfaces to guarantee that the sensor is as close as conceivable to the observed surface.
- The warmth created amid the solidifying of the polyester resign delivers a shift in the Bragg wavelength.
- The packaging design reduces the variation of coefficients of wavelength sensitivity by virtue of packaging process.

The output data gathered from fiber Bragg grating (FBG) sensor is actually an encoded wavelength i.e. by applying strain on Bragg gratings will cause a shift in peak wavelength of fiber Bragg grating sensor spectral response. To decode the information data, a device is required having ability to monitor

variations in wavelength precisely. Thus, optical spectrum analyzer is used to decode the information data obtained from FBG sensor.

An interrogation system is required to map the encoded data of wavelength to a power measurement. Various types of interrogation systems (filters) are available in the market such as an edge filters and arrayed-waveguide gratings. The working principle of these filters is very effective and easy to understand but the major drawback is the power conversion efficiency. The efficiency demultiplexed by an interrogation system is low, resulting in poor sensitivity of FBG sensor. To decrease the effects caused by interrogation systems such as small dynamic range, low sensitivity and to improve wavelength to power mapping, the bandwidth of fiber Bragg grating sensor is considered narrower than the bandwidth of interrogation system.

In this experiment, sm130 Optical Sensing Interrogator with wavelength of 1550-1590 nm was used because of its compact size, reliable design and long-term field operations. The experimental setup to monitor strain with FBG is shown in figure 4.1.

Figure 4.1 Experimental setup for strain monitoring

In this experiment, two iron rods were used: one rod was without corrosion and second rod was fully corroded as shown in figure 4.2. Both rods taken under consideration were identical in terms of dimensions i.e. they had 1.5-inch width, were 2 mm thick with length of 18 inch.

(a) (b)

Figure 4.2 (a) non-corroded iron rod, (b) corroded rod

One of the samples was manually corroded with the help of suitable synthetic chemicals available in the market. The list of chemicals, along with their quantities, used for the process of corrosion is given below:

- White vinegar (4 teaspoons)
- Hydrogen Peroxide (3 % - use a fresh bottle)
- Table salt (one-and-half teaspoons)
- Degreaser

The precision of the sensor was checked with test data in which the readings of the FBG sensor were contrasted and given by strain measures. The sensor was glued on the surface of both cement and iron samples. Then to analyse the as fabricated sensor, it was subjected to uniform tension, bending and compression. The readings of the FBG sensors were fundamentally the same as those of the strain checks. The experiment was performed by applying different amounts of loads on the rods under observation and the shift in wavelength was recorded via a computational machine.

4.4 RESULTS AND DISCUSSIONS

It was clearly observed from the results that when no load was applied, there was no shift in the Bragg wavelength (λ_B) of fiber Bragg grating sensor as shown in figure 4.3. A compression machine was used to apply different number of loads on the both iron rods which caused variations in the refractive index of FBG gratings. Due to variations in the refractive index of Bragg gratings, a shift in central wavelength of FBG spectrum was observed. Basically, this experiment was performed to analyse the effect of strain on structures and to enhance the performance of specially designed FBG sensor. For this reason, iron rods were considered as structural samples in this operation.

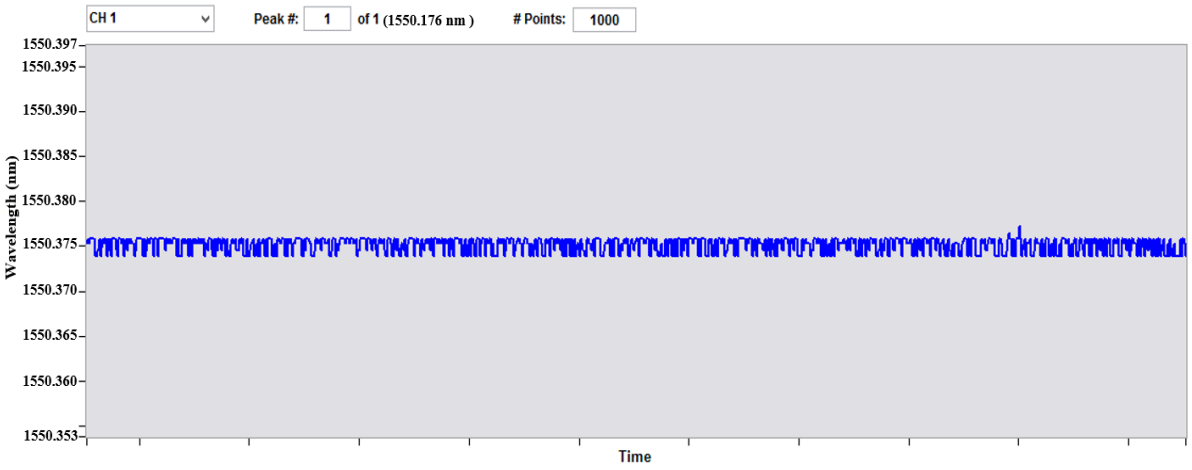

Figure 4.3 Reference wavelength

Here, different values of load are applied to verify the results. Based on the applied load, a particular change in Bragg wavelength has been demonstrated in the following graphs. The FBG sensor taken under inspection possess centred wavelength of 1550.376 nm by default. The graphs revealing the resultant values tested on non-corroded iron rod are shown in Fig 4.4 (a)-(c).

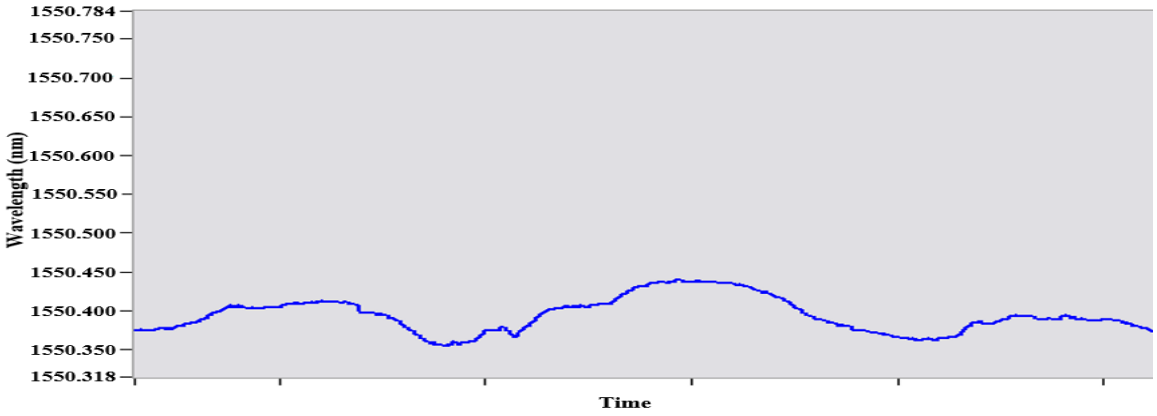

(a)

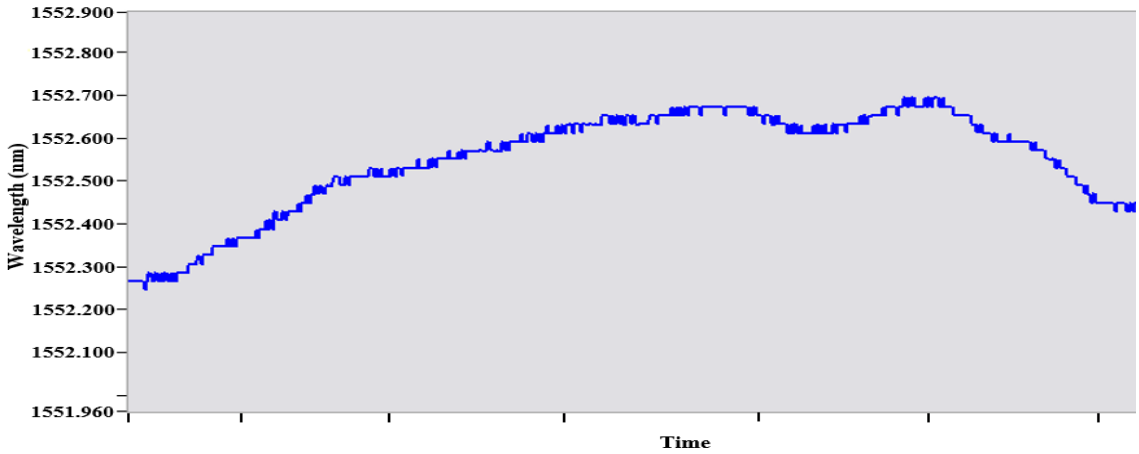

(b)

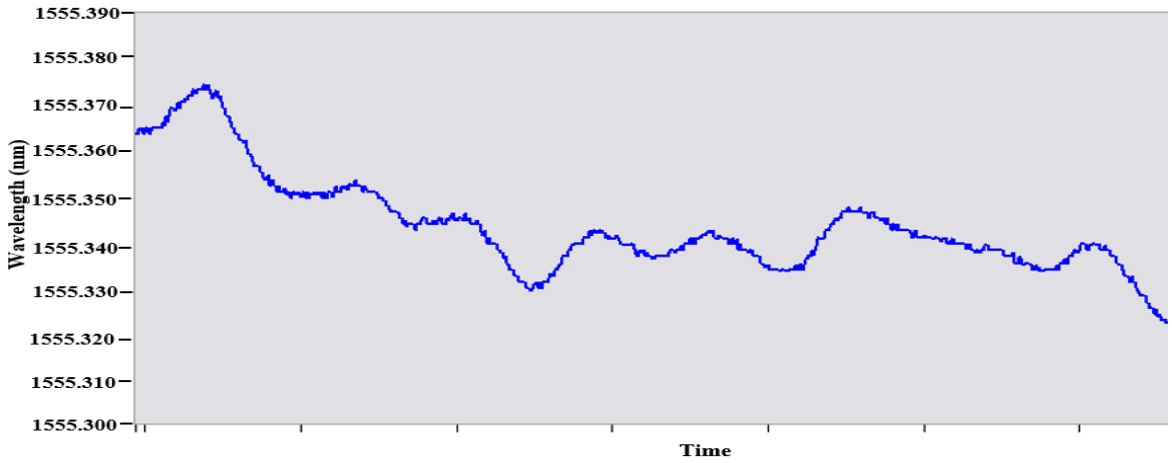

(c)

Figure 4.4 Variation in wavelength when (a) 5 kN load applied, (b) 30 kN load applied (c) 60 kN load applied.

When the load of 5 kN was applied on the non-corroded iron rod, a wavelength shift of 0.420 nm was observed, as revealed in Fig. 4 (a), while application of 30 kN, 60 kN load on the same sample showed shift of 2.540 nm, 5.132 nm Bragg wavelength was recorded. The shift of 5 nm in Bragg wavelength revealed that the sensitivity of FBG sensor has been enhanced.

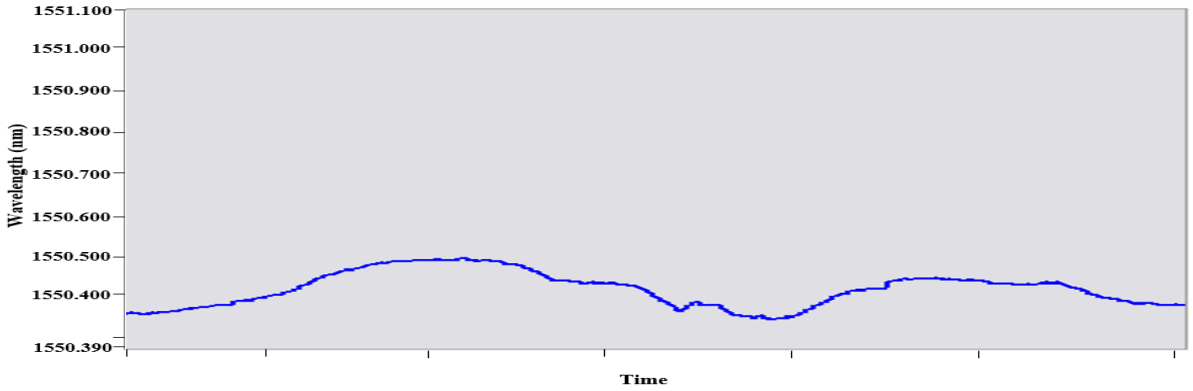

(a)

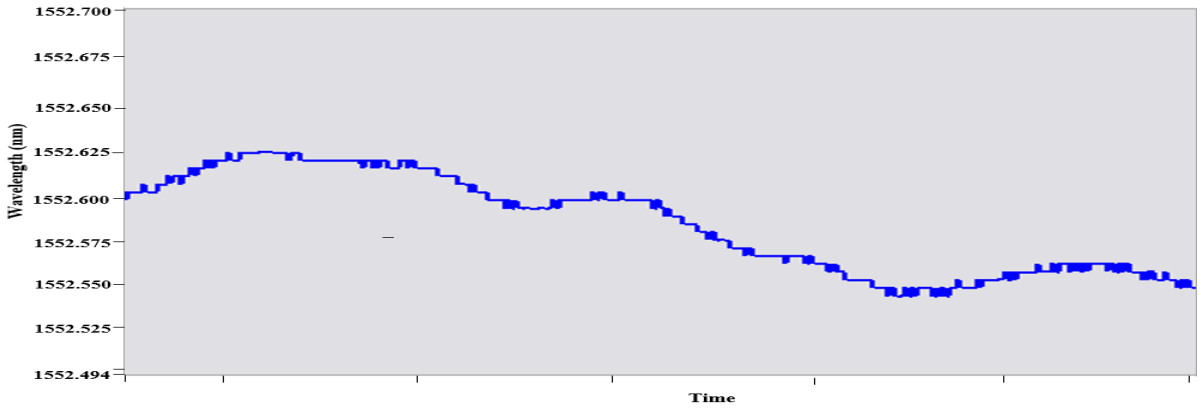

(b)

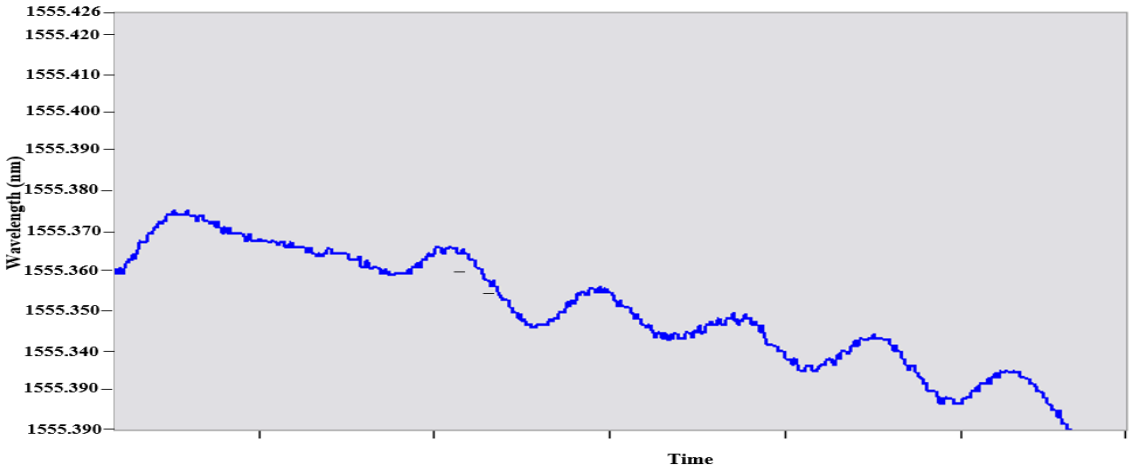

(c)

Figure 4.5 Variation in wavelength when (a) 5 kN load applied, (b) 15 kN load applied, (c) 30 kN load applied.

Then another rod (corroded) was analysed with same setup and under same default conditions. Then the results as obtained while testing strain measurement on corroded iron rods are shown in Fig. 4.5 (a) - (c).

The shift in Bragg wavelength of FBG spectrum of 0.82842 nm was recorded on application of 5 kN load. The shift increased to 2.62641 nm when 15 kN load was applied. But when 30 kN load was applied, the shift further increased to 5.3749 nm. Hence, the sensitivity of FBG sensor was found to be increased as the Bragg wavelength shifted from 1550.375 nm to 1555.3749 nm.

Figure 4.6 exhibited the bar graph depicting the difference in shift of Bragg wavelength for both samples (corroded and non-corroded iron rod) recorded to measure the value of applied strain.

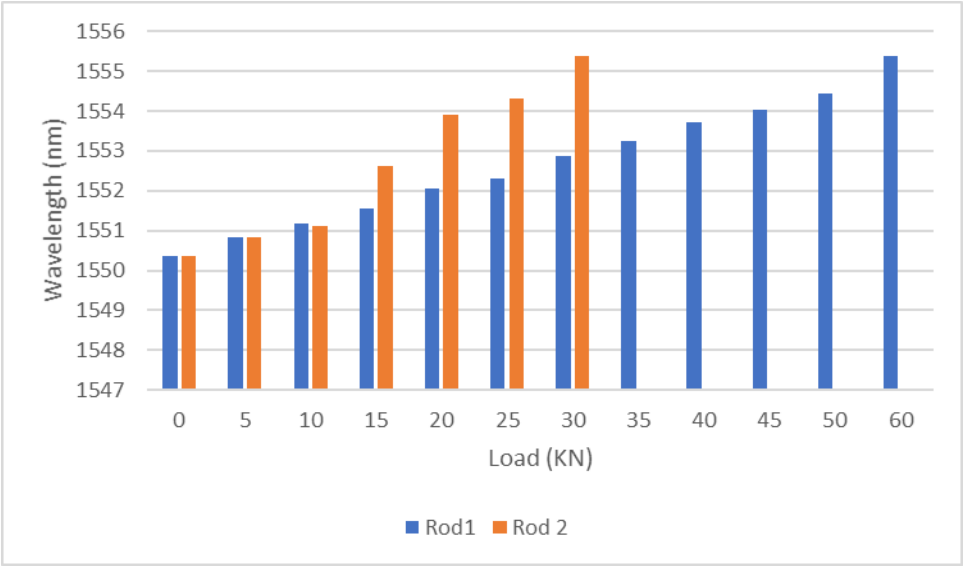

Figure 4.6 Wavelength shift as a function of applied load.

The following bar graph revealed that the 30 kN load was enough for the corroded rod to bear, it showed max reflection at this point and no further deflection in peak wavelength of FBG sensor was recorded when load of value above 30 kN was applied. Whereas, the non-corroded rod showed better mechanical strength in comparison to the former rod as it was able to bear a load up to the value of 60 kN and a max. deflection of 5 nm was observed there. These results suggested that the sensitivity of FBG sensor has been enhanced, attributing to the fact that now this sensor was able to measure the wavelength of 1555.357 nm.

4.5 CONCLUSION

It is concluded from the results that the proposed FBG sensor is very effective to monitor strain for two types of iron rods: one is non-corrosion and second is corroded rod. The system exhibited high stability and high sensitivity. The strain values were calculated by measuring the shift in Bragg wavelength of FBG sensor, when load was applied. For non-corroded rod, the maximum shift in wavelength was recorded to be 5 nm when 60 kN load was applied. For corroded rod, the maximum shift in wavelength was recorded of 4.9 nm when 30 kN load was applied. The proposed FBG sensor is highly recommended to measure strain for both non-corroded rods and corroded rods and could also be potentially used in the myriad of applications in civil domain.

CHAPTER-5

FUTURE SCOPE

The as-proposed optical sensor was successfully able to monitor the strength of metal rods based on the value of stress applied via observing shift in central Bragg wavelength. This sensor exhibited at best 5nm shift in wavelength. So, the potential of this sensor in practical structural health monitoring for massive structures could not be ignored.

1. It could be used to depict the variations in physical parameters in pipes, poles, pillars or rods for monitoring their health for civil applications. The desired shift in wavelength is possible to attain in this sensor with a little optimisation in refractive index plus by introducing different dimensions and change in number of gratings.
2. Further, to increase the sensitivity of sensor along with reduced variations in central wavelength, bandwidth and reflectivity for longer durations, various polymers such as polymethyl methacrylate (PMMA) and polycarbonate could be introduced. To reduce the fiber inscription time for accurate real time measurement recording, Benzyl dimethyl ketal (BDK) could be instigated inside the optical fiber.
3. Moreover, to reduce or terminate variation in temperature, two parallel sensors could be implanted. Based on the principle that one measures temperature variation as per the wavelength shift and other measures both temperature and strain; it would become possible to record alone strain variations by abolishing cross-sensitivity.

REFRENCES

[1] K. C. Kao and G. A. Hockham. Dielectric-fiber surface waveguides for optical frequencies. Proc. IEE, 113(7):1151–1158, 1966.

[2] F. T. S. Yu and S. Yin. Fiber Optic Sensors. Marcel Dekker, Inc., New York, 76:183-234, 2002.

[3] V. Vali and R. W. Shorthill. Fiber ring interferometer. Applied Optics, 15(5):1099–1100, 1976.

[4] P. Hariharan. Sagnac or Michaelson-Sagnac interferometer. Applied Optics, 14(10):2319–2321, 1975.

[5] T. Kumagai, H. Soekawa, T. Yuhara, and H. Kajioka. Fiber optic gyroscopes for vehicle navigation systems. Proceedings of SPIE, 2070:181–191, 1994.

[6] G. A. Sanders, B. Szafraniec, R. Y. Liu, C. Laskoskie, and L. Strandjord. Fiber optic gyros for space, marine and aviation applications. Proceedings of SPIE, 2837:61–71, 1996.

[7] G. A. Sanders and B. Szafraniec. Progress in fiber-optic gyroscope applications II with emphasis on the theory of depolarized gyros. AGARD/NATO Conference Report on Optical Gyros and Their Applications, 339:11–42, 1998.

[8] P. Shajenko, J. P. Flatley, and M. B. Moffett. On fiber-optic hydrophone sensitivity. Journal of the Acoustical Society of America, 64(5):1286–1288, 1978.

[9] H. L. Price. On the mechanism of transduction in optical fiber hydrophones. Journal of the Acoustical Society of America, 66(4):976–979, 1979.

[10] H. Nakstad and J. T. Kringlebotn. Oil and gas applications: Probing oil fields. Nature Photonics, 2(3):147–149, 2008.

[11] L. Zou, X. Bao, F. Ravet, and L. Chen. Distributed Brillouin fiber sensor for detecting pipeline buckling in an energy pipe under internal pressure. Applied Optics, 45(14):3372–3377, 2006.

[12] L. Zou, G. A. Ferrier, S. Afshar V., Q. Yu, L. Chen, and X. Bao. Distributed Brillouin scattering sensor for discrimination of wall-thinning defects in steel pipe under internal pressure. Applied Optics, 43(7):1583–1588, 2004.

[13] X. Bao, E. Ponomarev, Y. Li, F. Ravet, L. Zou, and O. M. Sezerman. Distributed Brillouin sensor system based on DFB lasers using offset locking. United States Patent, US 7,499,151 B2, 2009.

[14] L. Zou and O. M. Sezerman. Method and system for simultaneous measurement of strain and temperature. United States Patent, US 7,599,047 B2, 2009.

[15] S. C. Huang, W. W. Lin, M. T. Tsai, and M. H. Chen. Fiber optic in-line distributed sensor for detection and localization of the pipeline leaks. Sensors and Actuators A, 135:570–579, 2007.

[16] R. Bernini, A. Minardo, and L. Zeni. Vectorial dislocation monitoring of pipelines by use of Brillouin-based fiber-optics sensors. Smart Materials and Structures, 17(1):015006, 2008.

[17] L. Zou, X. Bao, S. Afshar V., and L. Chen. Dependence of the Brillouin frequency shift on strain and temperature in a photonic crystal fiber. Optics Letters, 29(13):1485–1487, 2004.

[18] L. Zou, X. Bao, Y. Wan, and L. Chen. Coherent probe-pump-based Brillouin sensor for centimeter-crack detection. Optics Letters, 30(4):370–372, 2005.

[19] W. Li, X. Bao, Y. Li, and L. Chen. Differential pulse-width pair BOTDA for high spatial resolution sensing. Optics Express, 16(26):21616–21625, 2008.

[20] H. Liang, W. Li, N. linze, L. Chen, and X. Bao. High-resolution DPP-BOTDA over 50 km LEAF using return-to-zero coded pulses. Optics Letters, 35(10):1503–1505, 2010.

[21] M. Jones. Structural-health monitoring: A sensitive issue. Nature Photonics, 2(3):153–154, 2008.

[22] X. Bao, C. Zhang, W. Li, M. Eisa, S. El-Gamal, and B. Benmokrane. Monitoring the distributed impact wave on a concrete slab due to the traffic based on polarization dependence on stimulated Brillouin scattering. Smart Materials and Structures, 17(1):015003, 2008.

[23] X. B´evenot, A. Trouillet, C. Veillas, H. Gagnaire, and M. Cl´ement. Hydrogen leak detection using an optical fiber sensor for aerospace applications. Sensors and Actuators B, 67:57–67, 2000.

[24] J. C. Juarez and H. F. Taylor. Polarization discrimination in a phase-sensitive optical time-domain reflectometer intrusion-sensor system. Optics Letters, 30(24):3284–3286, 2005.

[25] J. C. Juarez and H. F. Taylor. Field test of a distributed fiber-optic intrusion sensor system for long perimeters. Applied Optics, 46(11):1968–1971, 2007.

[26] Z. Zhang and X. Bao. Continuous and damped vibration detection based on fiber diversity detection sensor by Rayleigh backscattering. Journal of Lightwave Technology, 26(7):832–838, 2008.

[27] Z. Zhang and X. Bao. Distributed optical fiber vibration sensor based on spectrum analysis of polarization-OTDR system. Optics Express, 16(14):10240–10247, 2008.

[28] Q. Sun, D. Liu, J. Wang, and H. Liu. Distributed fiber-optic vibration sensor using a ring Mach-Zehnder interferometer. Optics Communications, 281(6):1538–1544, 2008.

[29] E. Pinet. Medical applications: Saving lives. Nature Photonics, 2(3):150–152, 2008.

[30] M. E. Bosch, A. J. R. S´anchez, F. S. Rojas, and C. B. Ojeda. Recent development in optical fiber biosensors. Sensors, 7:797–859, 2007.

[31] R. Wolthuis, D. McCrae, E. Saaski, J. Hartl, and G. Mitchell. Development of a medical fiber-optic pH sensor based on optical absorption. IEEE Transactions on Biomedical Engineering, 39(5):531–537, 1992.

[32] R. A. Wolthuis, D. McCrae, J. C. Hartl, E. Saaski, G. L. Mitchell, K. Garcin, and R. Willard. Development of a medical fiber-optic oxygen sensor based on optical absorption change. IEEE Transactions on Biomedical Engineering, 39(2):185–193,1992.

[33] P. A. E. Piunno, U. J. Krull, R. H. E. Hudson, M. J. Damha, and H. Cohen. Fiber optic biosensor for fluorimetric detection of DNA hybridization. Analytica Chimica Acta, 288(3):205–214, 1994.

[34] P. A. E. Piunno, U. J. Krull, R. H. E. Hudson, M. J. Damha, and H. Cohen. Fiber-Optic DNA sensor for fluorometric nucleic acid determination. Analytical Chemistry,67.

[35] Y. Zhang, X. Chen, Y. Wang, K. L. Cooper, and A. Wang. Microgap multicavity Fabry-P´erot biosensor. Journal of Lightwave Technology, 25(7):1797–1804, 2007.

[36] A. D. Kersey, M. A. Davis, H. J. Patrick, M. LeBlanc, K. P. Koo, C. G. Askins, M. A. Putnam, and E. J. Friebele. Fiber grating sensors. Journal of Lightwave Technology, 15(8):1442–1463, 1997.

[37] C. E. Lee, H. F. Taylor, A. M. Markus, and E. Udd. Optical-fiber Fabry-Perot embedded sensor. Optics Letters, 14(21):1225–1227, 1989.

[38] B. Dong, L. Wei, and D. P. Zhou. Miniature high-sensitivity high-temperature fiber sensor with a dispersion compensation fiber-based interferometer. Applied Optics, 48(33):6466–6469, 2009

[39] M. G. Xu, H. Geiger, J. L. Archambault, L. Reekie, and J. P. Dakin. Novel interrogating system for fiber Bragg grating sensors using an acousto-optic tunable filter. Electronics Letters, 29(17):1510–1511, 1993.

[40] A. D. Kersey, M. A. Davis, and D. Bellemore. Development of fiber sensors for structural monitoring. Proceedings of SPIE, 2456:262–268, 1995.

[41] M. A. Davis, D. G. Bellemore, T. A. Berkoff, and A. D. Kersey. Design and performance of a fiber Bragg grating distributed strain sensor system. Proceedings of SPIE, 2446:227–235, 1995.

[42] M. A. Davis and A. D. Kersey. Matched-filter interrogation technique for fiber Bragg grating arrays. Electronics Letters, 31(10):822–823, 1995

[43] A. H. Hartog. A distributed temperature sensor based on liquid-core optical fibers. Journal of Lightwave Technology, 1(3):498–509, 1983.

[44] J. P. Dakin, D. J. Pratt, G. W. Bibby, and J. N. Ross. Distributed optical fiber Raman temperature sensor using a semiconductor light source and detector. Electronics Letters, 21(13):569–570, 1985.

[45] X. Bao, D. J. Webb, and D. A. Jackson. 22-km distributed temperature sensor using Brillouin gain in an optical fiber. Optics Letters, 18(7):552–554, 1993.

[46] O. Fraz˜ao, J. M. Baptista, and J. L. Santos. Recent advantages in high-birefringence fiber loop mirror sensors. Sensors, 7(11):2970–2983, 2007.

[47] R. Kashyap. Fiber Bragg gratings. Elsevier Academic Press, San Diego, 1999.

[48] K. O. Hill, Y. Fujii, D. C. Johnson, and B. S. Kawasaki. Photosensitivity in optical fiber waveguides: Application to reflection filter fabrication. Applied Physics Letters, 32(10):647–649, 1978.

[49] J. Stone. Photorefractivity of GeO2-doped silica fibers. Journal of Applied Physics, 62(11):4371–4374, 1987.

[50] F. P. Payne. Photorefractive gratings in single-mode optical fibers. Electronics Letters, 25(8):498–499, 1989.

[51] G. Meltz, W. W. Morey, and W. H. Glenn. Formation of Bragg gratings in optical fibers by a transverse holographic method. Optics Letters, 14(15):823–825, 1989.

[52] D. P. Hand and P. St. J. Russell. Photoinduced refractive-index changes in germanosilicate fibers. Optics Letters, 15(2):102–104, 1990.

[53] R. Kashyap. Photosensitive optical fibers: Devices and applications. Opticical Fiber Technology, 1(1):17–34, 1994.

[54] G. Keiser. Optical Fiber Communications. The McGraw-Hill Companies, Inc., United States, 3rd edition, 2000.

[55] A. M. Vengsarkar, P. J. Lemaire, J. B. Judkins, V. Bhatia, T. Erdogan, and J. E. Sipe. Long-period fiber gratings as band-rejection filters. In Tech. Dig. Conf. Opt. Fiber Commun., pages Postdeadline paper PD4–2, Sandiego, CA, 1995.

[56] A. D. Kersey, M. A. Davis, H. J. Patrick, M. LeBlanc, K. P. Koo, C. G. Askins, M. A. Putnam, and E. J. Friebele. Fiber grating sensors. Journal of Lightwave Technology, 15(8):1442–1463, 1997.

[57] A. M. Vengsarkar, P. J. Lemaire, J. B. Judkins, V. Bhatia, T. Erdogan, and J. E. Sipe. Long-period fiber gratings as band-rejection filters. Journal of Lightwave Technology, 21(1):58–65, 1996.

[58] A. M. Vengsarkar, J. R. Pedrazzani, J. B. Judkins, P. J. Lemaire, N. S. Bergano, and C. R. Davidson. Long-period fiber-grating-based gain equalizers. Optics Letters, 21(5):336–338, 1996.

[59] V. Bhatia and A. M. Vengsarkar. Optical fiber long-period grating sensors. Optics Letters, 21(9):692–694, 1996.

[60] H. J. Patrick, G. M. Williams, A. D. Kersey, J. R. Pedrazzani, and A. M. Vengsarkar. Hybrid fiber Bragg grating/long period fiber grating sensor for strain/temperature discrimination. IEEE Photonics Technology Letters, 8(9):1223–1225, 1996.

[61] V. Bhatia, K. A. Murphy, R. O. Claus, and A. M. Vengsarkar. Simultaneous measurement systems employing long-period grating sensors. In Optical Fiber Sensors, Sapporo, Japan, paper Fr25, 1996.

[62] Y. Y. Shevchenko and J. Albert. Plasmon resonances in gold-coated tilted fiber Bragg gratings. Optics Letters, 32(3):211–213, 2007.

[63] T. Guo, A. Ivanov, C. Chen, and J. Albert. Temperature-independent tilted fiber grating vibration sensor based on cladding-core recoupling. Optics Letters, 33(9):1004– 1006, 2008

[64] T. Guo, H. Y. Tam, P. A. Krug, and J. Albert. Reflective tilted fiber Bragg grating refractometer based on strong cladding to core recoupling. Optics Express, 17(7):5736–5742, 2009

[65] Y. X. Jin, C. C. Chan, X. Y. Dong, and Y. F. Zhang. Temperature-independent bending sensor with tilted fiber Bragg grating interacting with multimode fiber. Optics Communications, 282(19):3905–3907, 2009.

[66] F. Ouellette. All-fiber filter for efficient dispersion compensation. Optics Letters, 16(5):303–305, 1991.

[67] K. C. Byron, K. Sugden, T. Bricheno, and I. Bennion. Fabrication of chirped Bragg gratings in photosensitive fiber. Electronics Letters, 29(18):1659–1660, 1993.

[68] P. C. Hill and B. J. Eggleton. Strain gradient chirp of fiber Bragg gratings. Electronics Letters, 30(14):1172–1174, 1994.

[69] M. A. Putnam, G. M. Williams, and E. J. Friebele. Fabrication of tapered, strain gradient chirped fiber Bragg gratings. Electronics Letters, 31(4):309–310, 1995.

[70] A. Othonos, X. Lee, and R. M. Measures. Superimposed multiple Bragg gratings. Electronics Letters, 30(23):1972–1974, 1994

[71] B. G. Eggleton, P. A. Krug, L. Poladian, and F. Ouellette. Long periodic superstructure Bragg gratings in optical fibers. Electronics Letters, 30(19):1620–1622, 1994

[72] L. A. Ferreira, F. M. Ara´ujo, J. L. Santos, and F. Farahi. Simultaneous measurement of strain and temperature using interferometrically interrogated fiber Bragg grating sensors. Optical Engineering, 39(8):2226–2234, 2000.

[73] S. W. James, M. L. Dockney, and R. P. Tatam. Simultaneous independent temperature and strain measurement using in-fiber Bragg gratings sensors. Electronics Letters, 32(12):1133–1134, 1996.

[74] P. M. Cavaleiro, A. M. Ara´ujo, L. A. Ferreira, J. L. Santos, and F. Farahi. Simultaneous measurement of strain and temperature using Bragg gratings written in germanosilicate and boron-codoped germanosilicate fibers. IEEE Photonics Technology Letters, 11(12):1635–1637, 1999.

[75] R. Aashiam and S. Asokan. Simultaneous measurement of strain and temperature using type I and pre-strained fiber bragg grating. Sensors, 2009 IEEE:1229-1231, 2009.

[76] A. Kerrouche, W. J. O. Boyle, T. Sun, K. T. V. Grattan, J. W. Schmidth and B. Taljsten. Strain measurement using embedded fiber bragg grating sensors inside an anchored carbon fiber polymer reinforcement prestressing rod for structural monitoring. IEEE Sensors Journal, 9(11):1456-1461, 2009.

[77] G. S. Hwang, D. W. Huang and C. C. Ma. Numerical study on strain measurements using the improved bonding fiber bragg grating. IEEE Sensors Journal, 10(5):1012-1018, 2010.

[78] M. I. Comanici, L. R. Chen, P. Kung and L. Wang. Measurement of dynamic strain using a fiber bragg grating-based laser sensor system. 2011 ICO International Conference on Information Photonics (IP), IEEE: 1-2, 2011.

[79] Y. Shinoda, T. Arai, D. Miyata and T. Higo. Real-time measurement of static strain using fiber bragg grating with optical frequency domain reflectometry. SICE Annual Conference 2011, IEEE: 1870-1873, 2011.

[80] Y. Mizutani and R. M. Groves. Multi-functional measurement using a single FBG sensor. Experimental Mechanics, 51:1489-1498, 2011.

[81] R. Bader, T. Pagel, H. Renner and E. Brinkmeyer. Characterization of chirped fiber bragg gratings: Identification and removal of cladding-mode perturbations in measurement data, Journal of lightwave technology, 29(12):1783-1789, 2011.

[82] Y. Shinoda, M. Yamada, T. Arai, T. Higo. Static strain measurement by fiber bragg gratings using multiplexed common-path interferometers. SICE Annual Conference 2012, IEEE: 1021-1024, 2012.

[83] D. Wada, H. Murayama and H. Igawa. Lateral load measurements based on a distributed sensing system of optical frequency-domain reflectometry using long-length fiber bragg gratings. Journal of Lightwave Technology, 30(14): 2337-2344, 2012.

[84] W. Qui, X. Cheng, Y. Luo, Q. Zhang and B. Zhu. Simultaneously measurement of temperature and strain using a single bragg grating in a few-mode polymer optical fiber. Journal of Lightwave Technology, 31(14): 2419-2425, 2013.

[85] N. Kuse, A. Ozawa and Y. Kobayashi. Static fiber bragg grating strain sensor with high resolution and large dynamic range by dual-comb spectroscopy. Optic Express, 21(9): 11141-11149, 2013.

[86] J. Du and Z. He. Sensitivity enhanced strain and temperature measurements based on FBG and frequency chirp magnification. Optic Express, 21(22): 27111-27118, 2013.

[87] L. Xian, P. Wang and H. Li. Simultaneous temperature and strain measurement by using a wide-band fiber bragg grating. Optoelectronics and Communications Conference held jointly with 2013 International Conference on Photonics in Switching (OECC/PS), IEEE, 18:1-2, 2013.

[88] S. W. Choi, J. Lee, B. H. Oh and H. S. Park. Measurement model for the maximum strain in beam structures using multiplexed fiber bragg grating sensors. International Journal of Distributed Sensor Networks 9(10): 894780,2013

[89] W. Zhang, W. Chen, Y. Shu, X. Lei and X. Liu. Effects of bonding layer on the available strain measuring range of fiber Bragg gratings. Applied Optics 53(5): 885-891.2014.

[90] X. Hu, C. F. J. Pun, H. Y. Tam, P. Megret and Christophe. Highly reflective Bragg gratings in slightly etched step-index polymer optical fiber. Optics express 22(15): 18807-18817, 2014.

[91] J. Shi, M. Tang, S. Fu and D. Liu Modeling and Analysis of Fiber Bragg Grating Based Visible Pr^{3+}-Doped Fiber Lasers. Journal of Lightwave Technology, 32(1), 27-34.

[92] C. C. Chiang, and C. C. Tseng. Characterization of notched long-period fiber gratings: effects of periods, cladding thicknesses, and etching depths. Applied optics 53(20): 4398-4404, 2012.

[93] R. Oliveira, L. Bilro and R. Nogueira. Bragg gratings in a few mode microstructured polymer optical fiber in less than 30 seconds. Optics express 23(8): 10181-10187, 2015.

[94] W. Shen, R. Yan, L Xu. Application study on FBG sensor applied to hull structural health monitoring. Optik-International Journal for Light and Electron Optics 126(17): 1499-1504, 2015.

[95] J. Chen, Q. Liu, X. Fan and Z. He. Simultaneous measurement of strain and temperature using pi-phase-shifted Fiber Bragg grating on polarization maintaining fiber. OptoElectronics and Communications Conference (OECC) held jointly with 2016 International Conference on Photonics in Switching (PS), IEEE, 21:1-3, 2016.

[96] J. Kong, X. Quyang, A. Zhou, H. Yu and L. Yuan. Pure directional bending measurement with a fiber Bragg grating at the connection joint of eccentric-core and single-mode fibers. Journal of Lightwave Technology 34(14): 3288-3292, 2016.

[97] K. Fröjdh, G. Hedin, and S. Helmfrid. Strain and temperature measurement using a 9.5-m continuous chirped fiber Bragg grating with millimeter resolution. Optical Fiber Sensors Conference (OFS), IEEE, 25th.:1-4, 2017.

[98] M. Zhu, and H. Murayama. Simultaneous measurement of dynamic strain and temperature distribution using high birefringence PANDA fiber Bragg grating. Optical Fiber Sensors Conference (OFS), 2017 25th. IEEE:1-4, 2017.

[99] A. Pospori, and D. J. Webb. Stress Sensitivity Analysis of Optical Fiber Bragg Grating-Based Fabry–Pérot Interferometric Sensors. Journal of Lightwave Technology 35(13): 2654-2659, 2017.

[100] J. Chen, Q. Liu and Z. He. High resolution simultaneous measurement of strain and temperature using pi-phase-shifted FBG in polarization maintaining fiber. Journal of Lightwave Technology 35(22): 4838-4844, 2017.

[101] A. Pospori, C.A.F. Marques, O. Bang, D. J. Webb and P. Andre. Polymer optical fiber Bragg grating inscription with a single UV laser pulse. Optics express 25(8): 9028-9038, 2017.

[101] R. Xing, C. Dong, Z. Wang, Y. Wu, Y. Yang and S. Jian. Simultaneous strain and temperature sensor based on polarization maintaining fiber and multimode fiber. Optics and Laser Technology, 102: 17-21, 2018.

[102] J. Kumar and D. Chack. FBG based sensor with temperature compensation for structural health monitoring. 2018 4th International Conference on Recent Advances in Information Technology (RAIT). IEEE: 1-4, 2018.

[103] A. L. Aldaba, J. L. Auguste, R. Jamier, P. Roy and M. L. Amo. Simultaneous strain and temperature multipoint sensor based on microstructured optical fiber. Journal of Lightwave Technology 36(4): 910-916, 2018.

[104] A. Wada, S. Tanaka and N. Takahashi. Fast and high-resolution simultaneous measurement of temperature and strain using a fabry-perot interferometer in polarization-maintaining fiber with laser diodes. Journal of Lightwave Technology 36(4): 1011-1017, 2018.

[105] C. A. F. Marques, R. Min, A. L. Junior, P. Antunes, A. Fasano, G. Woyessa, K. Nielsen, H. K. Rasmussen, B. Ortega, and O. Bang. Fast and stable gratings inscription in POFs made of different materials with pulsed 248 nm KrF laser. Optics Express, 26(2): 2013-2022, 2018.

[106] C. Lu, J. Su, X. Dong, T. Sun and K. T. V. Grattan. Simultaneous measurement of strain and temperature with a few mode fiber-based sensor. Journal of Lightwave Technology, 36(13): 2796-2802, 2018.

[107] A. K. Garg, R. S. Kaler. Performance analysis of an integrated scheme in optical burst switching high-speed networks, Chinese Optics Letters 6 (4), 244-247.

[108] K. S. Bhatia, R. S. Kaler, T. S. Kamal and R. Randhawa. Simulative analysis of integrated DWDM and MIMO-OFDM system with OADM, OPTIK-International journal for Light and electron Optics 124 (2), 117-121.

[109] A. Wason and R. S. Kaler. Wavelength assignment algorithms for WDM optical networks, Optik-International Journal for Light and Electron Optics 122 (10), 877-880.

[110] J. Malhotra, A. K. Sharma and R. S. Kaler. On the performance analysis of wireless receiver using generalized-gamma fading model, annals of telecommunications-annales des télécommunications 64 (1-2), 147-153.

[111] R. S. Kaler, T. S. Kamal, A. K. Sharma, S. K. Arya and R. A. Agarwal. Large signal analysis of FM-AM conversion in dispersive optical fibers for PCM systems including second order dispersion, Fiber &Integrated Optics 21 (3), 193-203.

[112] S. Singh and R. S. Kaler. Investigation of hybrid optical amplifiers with different modulation formats for DWDM optical communication system, Optik-International Journal for Light and Electron Optics 124 (15), 2131-2134.

[113] S. Singh and R. S Kaler. Placement of optimized semiconductor optical amplifier in fiber optical communication systems, Optik-International Journal for Light and Electron Optics 119 (6), 296-302.